AD-A094 739 BATTELLE COLUMBUS LABS OH F/G 7/4
AN INVESTIGATION OF THE EFFECTS OF OXYGEN AND WATER VAPOR ON TH--ETC(U)
DEC 80 E DRAUGLIS, D K SNEDIKER AFOSR-76-3051
UNCLASSIFIED AFOSR-TR-81-0036 NL

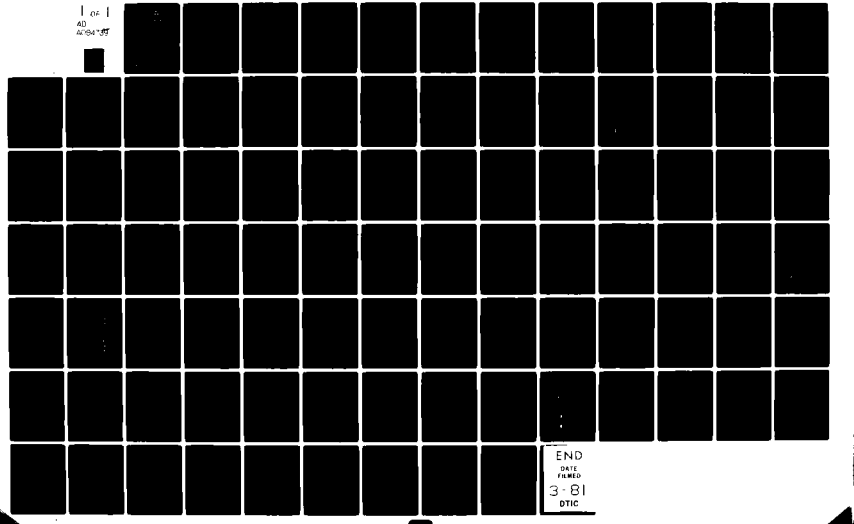

Battelle
Columbus Laboratories

LEVEL II

Report

FINAL REPORT

on

AN INVESTIGATION OF THE EFFECTS OF OXYGEN AND WATER VAPOR ON THE COMPRESSIVE FILM STRENGTH OF BOUNDARY FILMS ON IRON SUBSTRATES.

to

DEPARTMENT OF THE AIR FORCE
OFFICE OF SCIENTIFIC RESEARCH

December 31, 1980

by

E. Drauglis
D. K. Snediker

BATTELLE
Columbus Laboratories
505 King Avenue
Columbus, Ohio 43201

Unclassified

SECURITY CLASSIFICATION OF THIS PAGE (When Data Entered)

REPORT DOCUMENTATION PAGE		READ INSTRUCTIONS BEFORE COMPLETING FORM
1. REPORT NUMBER **AFOSR-TR- 81-0036**	2. GOVT ACCESSION NO. AD-A094 739	3. RECIPIENT'S CATALOG NUMBER
4. TITLE (and Subtitle) An Investigation of the Effects of Oxygen and Water Vapor on the Compressive Film Strength of Boundary Films on Iron Substrates		5. TYPE OF REPORT & PERIOD COVERED Final 6/1/79 - 11/30/80
		6. PERFORMING ORG. REPORT NUMBER
7. AUTHOR(s) David J. Snediker and Edmund Drauglis		8. CONTRACT OR GRANT NUMBER(s) AFOSR-76-3051
9. PERFORMING ORGANIZATION NAME AND ADDRESS Battelle, Columbus Laboratories 505 King Avenue Columbus, Ohio 43201		10. PROGRAM ELEMENT, PROJECT, TASK AREA & WORK UNIT NUMBERS 61102F 2303/A2
11. CONTROLLING OFFICE NAME AND ADDRESS Air Force Office of Scientific Research/NC Bolling AFB, DC 20332		12. REPORT DATE December 31, 1980
		13. NUMBER OF PAGES 90
14. MONITORING AGENCY NAME & ADDRESS(if different from Controlling Office)		15. SECURITY CLASS (of this report) Unclassified
		15a. DECLASSIFICATION DOWNGRADING SCHEDULE

16. DISTRIBUTION STATEMENT (of this Report)

Approved for public release; distribution unlimited.

17. DISTRIBUTION STATEMENT (of the abstract entered in Block 20, if different from Report)

18. SUPPLEMENTARY NOTES

19. KEY WORDS (Continue on reverse side if necessary and identify by block number)

Lubrication	Tricresyl Phosphate
Lubricant chemistry	Ester
Surface chemistry	ESCA
Infrared spectroscopy	X-Ray Photoelectron Spectroscopy

20. ABSTRACT (Continue on reverse side if necessary and identify by block number)

The objectives of this program are to determine the effects of water and oxygen on the compressive strength of boundary lubricant films and to correlate these effects with the fundamental physical and chemical phenomena responsible for the formation and stabilization of the films and the inverse phenomena of degradation and dissolution.

Compressive film strengths were measured under controlled atmospheres by means of a unique film penetration apparatus developed at Battelle. All experiments

(Continued)

DD FORM 1 JAN 73 1473 EDITION OF 1 NOV 65 IS OBSOLETE

SECURITY CLASSIFICATION OF THIS PAGE (When Data Entered)

were performed on films formed from the diester di-2-ethylhexyl sebacate containing various amounts of tricresyl phosphate.

It was found that water is detrimental to the formation of good boundary films and that oxygen is necessary for the formation of good boundary films.

Scanning electron microscopy showed that nonmetallic inclusions on ARMCO iron surfaces play an important role in initiating the formation of strong boundary films. Experiments with inclusion-free zone refined iron verified this result.

Fourier transform infrared spectroscopy and X-ray photoelectron spectroscopy were also used to study the surface chemistry of the films. These techniques seem to indicate that the residual films are almost exclusively inorganic phosphates.

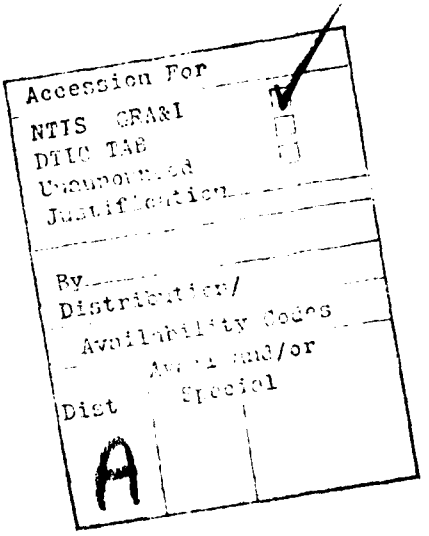

TABLE OF CONTENTS

LIST OF TABLES

LIST OF FIGURES

LIST OF FIGURES (Contd)

LIST OF FIGURES (Contd)

FINAL REPORT

on

AN INVESTIGATION OF THE EFFECTS OF OXYGEN AND WATER VAPOR ON THE COMPRESSIVE FILM STRENGTH OF BOUNDARY FILMS ON IRON SUBSTRATES

to

DEPARTMENT OF THE AIR FORCE
OFFICE OF SCIENTIFIC RESEARCH

December 8, 1980

I. INTRODUCTION

Most lubricated machine elements operate, at least in part, in the boundary regime in which very thin films having proper- ties significantly different from bulk fluids, are responsible for the effectiveness of the lubrication and the service life of the lubricated element. These critical boundary films are formed by complex physical and chemical interactions between a solid (usually metal) machine element, the lubrication fluid, and the ambient atmosphere. In the past decade, significant advances have been made in gaining an understanding of the chemistry of the interaction of many different types of additives, base oils, and various metal substrates.[1-7] However, relatively little effort has been expended on the study of the effects of ambient atmosphere on the formation and stabilization of boundary films. In particular, the most common and reactive substances found in the atmosphere, O_2 and H_2O, have been sadly neglected. In recent years, only Buckley[1], Fein[2], and Begelinger and DeGee[3] have made significant contributions to our understanding of the role of O_2 in the formation

of boundary lubricant films. However, much less work has been performed on the role of H_2O and almost no research has been performed on the combined effects of H_2O and O_2. The small amount of work performed on these substances suggests that their effects on lubricant films are large. However, the precise elucidation of the basic interactions occurring among H_2O, O_2, the lubricant, and the substrate requires much more research on well-characterized substrates and well-defined lubricating fluids.

About 4 years ago, a research program was initiated at BCL aimed at answering some of the basic questions relating to the role of H_2O and O_2 in lubricant films. The approach taken in this program was to study a fundamental mechanical property of the films - the compressive rupture strength. Well-characterized, well-purified lubricants and additives and well-characterized substrates were used. Rupture strength measurements were made on a unique film-penetration apparatus developed at BCL.[8] This apparatus is so constructed that a stylus may be incrementally loaded over a wide load range until film rupture, detected by electrical continuity, occurs.

In the first 2 years of the program, films formed from a diester, di-2-ethylhexyl sebacate, and solutions of tricresyl phosphate in the diester were studied. In addition to the film rupture strength measurements, ellipsometry and external reflection infrared spectroscopy were performed. In all experiments, the substrate was highly polished ARMCO iron. In the third year of the program, the effects of variations in oxygen and TCP concentration were studied in an effort to better understand the mechanisms involved in the formation of viable boundary films. In the fourth year of this program, in which the role of TCP concentration was determined, a potentially significant metallurgical factor was studied, and efforts were made to elucidate the chemistry of the iron/TCP/E105/O_2 system.

II. FILM STRENGTH STUDIES

Static compressive strength, the primary boundary film characterization parameter used in this research, was measured using a modified version of the apparatus described in Reference 8. The apparatus, the reagents, and the techniques used are described in detail in the following sections.

Apparatus

The apparatus has been heavily modified over the course of the research in order to enhance reproducibility and ease of operation. Figure 1 shows a schematic drawing of the apparatus in its final form. The flat specimen (substrate) rests on a heated stage that can be moved in the x-y directions by means of micrometer drives. The stylus - 0.0051 cm in diameter - is loaded against the specimen plate by means of a pneumatic load system. This system - totally different in concept that the employed previously - employs a Be-Cu bellows as a pneumatic actuator to press the stylus against the plate while reacting this load through a precision load cell. The rate of load application is determined by the rate of pressure increase in the bellows. This rate is adjusted by means of an adjustable leak in the pneumatic system. The system is actuated by opening and closing an exhaust valve. The work reported herein used a rate of load application of approximately 3 grams/sec - a rate chosen to minimize impact effects as the stylus approaches the surface. While the maximum load that this apparatus can apply to the stylus tip is well over 200 grams, we have limited the load to 160 grams in order to minimize damage to the stylus and the substrate.

Film rupture is detected electrically. The stylus-substrate interface is a part of an electrical circuit that imposes a

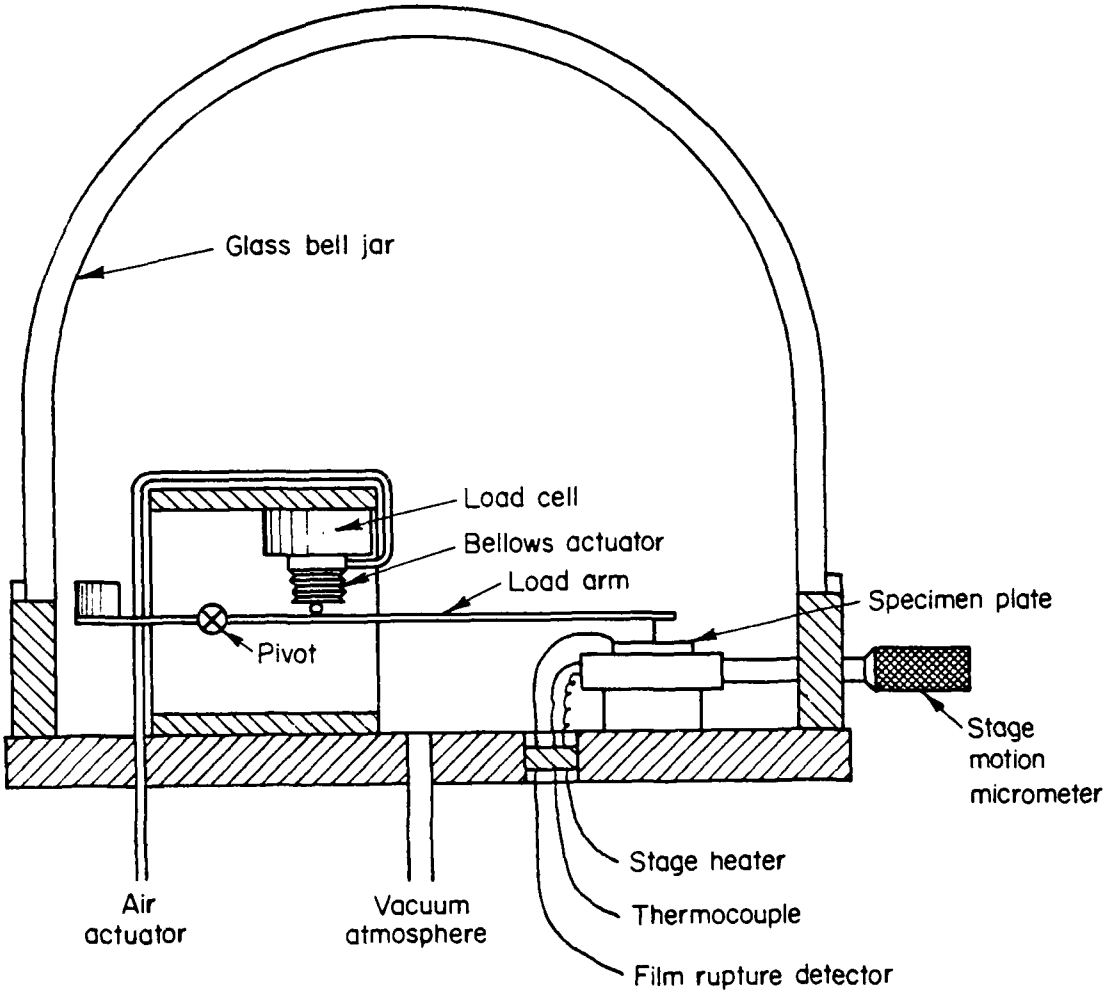

FIGURE 1. SCHEMATIC DRAWING OF THE MODIFIED APPARATUS

voltage of 1.6 across the interface and automatically trips at a preset resistance of 20 ohms. This trip load is automatically registered for readout. The constant application of load and the film rupture detection circuit eliminate two sources of experimental uncertainty associated with the earlier versions of this apparatus - constancy and smoothness of load application and reproducible identification of the point of film rupture. Reproducibility and drift of the electronic components involved were found to produce less than 1 percent variation in readings taken over many hours.

The entire apparatus is enclosed in a vacuum chamber provided with feed-throughs for mechanical motion, electrical signals, and the introduction of reactants, both liquid and gaseous. Liquid reactants are introduced via a vacuum-compensated additional funnel. The gaseous atmospheres are introduced via a stainless steel manifold under the vacuum chamber base plate. The purge gases exit through an oil bubbler against a head of approximately 10 cm oil.

The temperature of the iron specimen was measured by means of a thermocouple pressed by spring pressure against the specimen surface 1 cm away from the stylus contact point.

The styli used in these experiments were made of hardened carbon steel. They were first cleaned by tumbling in Al_2O_3 and then cleaned thoroughly with deionized H_2O and absolute ethyl alcohol. The styli were 100 percent microscopically inspected to ensure a tip radius of 0.0051 cm, a spherical geometry, and good surface finish.

Reactants

Surface Preparation

In most of the experiments described in this report, the substrate material was ARMCO iron. This material has the following properties:

- Composition:

C	Mn	P	S	Si	Fe
0.015	0.028	0.005	0.025	0.003	Balance

- Tensile strength: 42,000 psi
- Rockwell hardness: B40-50
- Modulus of elasticity: 30×10^6 psi.

After extensive experimentation with various finishing and cleaning techniques, including sputter etching, the following procedure was found to yield the most consistent and reproducible surfaces:

(1) Cut from bar stock and surface grind both sides flat

(2) Wet polish on metallographic papers through 600 grit

(3) Diamond lap

(4) Polish with a slurry of Glennel Diamond compound Type UB (0.5-1 μ size) in kerosene on a lintless rayon polishing cloth. Rinse with absolute ethanol.

(5) Rinse: tap H_2O
deionized H_2O

Absolute ethanol

Air dry.

This procedure is changed from that used earlier in the program. The Linde-B/H_2O polish final step was replaced by the diamond cloth polish. We found that this method yielded more reproducible initial surfaces as measured by our standard criterion of an average load-to-rupture of <1 gram prior to the introduction of any reactants. In the course of working out this new technique, it also was discovered that used plates must be run through Steps 2-4, not just the final polish, as has been done in the past. This suggests an extremely tenacious film that cannot be removed by a simple, light abrasion.

Lubricant Solutions

The liquid reactants used in these experiments were a diester of relatively high purity - 99 percent 2-ethylhexyl sebacate (E-105, 1 percent probably monoester) and technical grade tricresyl phosphate (TCP). The TCP contained essentially 25 percent each of the four isomers with two other components at the 2 percent level. For dry experiments, the E-105/TCP solutions were dried for at least 24 hours over a Linde type 5A molecular sieve. The dry solution was poured directly into the addition funnel which was immediately sealed and evacuated. For "wet" experiments, the dry solution was shaken with distilled water in a separatory funnel and the water-saturated organic phase drawn off for immediate use.

The gaseous environments, air and argon, were introduced into the system directly from the bottle via Tygon and stainless steel tubing. The air used with Matheson dry grade with a dew point of -75 F, maximum. The argon was Matheson UHP grade with a dew point of -90 F maximum and containing 1-2 ppm O_2 maximum. The Ar/O_2

mixtures were Matheson analyzed gases consisting of mixtures of 20.24% O_2 in Ar, 5.41% O_2 in Ar and 1.05% O_2 in Ar.

Experimental Procedures

Each experiment in controlled atmosphere was carried out according to the following sequence:

(1) The iron substrate was installed and the electrical connections made. The surface-contact thermocouple was put in place and checked out.

(2) A new stylus was installed.

(3) The bell jar was put in place.

(4) The E-105 solution, wet or dry, was placed in the addition funnel.

(5) The system was evacuated to a pressure of approximately 200 microns. The space above the liquid in the addition funnel was evacuated simultaneously.

(6) The system was back-filled with the appropriate atmosphere.

(7) Steps 5 and 6 were repeated five times.

(8) After the final purge, the controlled atmosphere was allowed to flow through the system for approximately 1 hour.

(9) Ten to twenty load-to-rupture measurements were made on the bare iron plate. If the average exceeded 5 grams, or if any high values (>20 grams) appeared, the experiment was aborted and the plate refinished.

The technique for making these measurements was the standard applied to all determinations: the readings were taken in rapid succession at surface sites 10 mils apart. These and subsequent measurements were generally taken in a straight line across and center portion of the plate. A standard series consisting of 2 to 22 measurements took less than 5 minutes.

(10) The liquid reactant was introduced and allowed to flow over the specimen plate in a thick film.

(11) Approximately ten to twenty measurements were taken with the plate at room temperature.

(12) The specimen plate was heated to the experimental temperature level...the heating rate being 2.3 C/minute. Input voltage was controlled to maintain the desired temperature.

(13) Once at temperature, an elapsed timer was started and a series of 10 to 20 load-to-rupture readings were taken. Subsequent readings were taken at 30 minute intervals, each set of 20 beginning at the specified elapsed time and taking 3 minutes to complete.

The gas was allowed to flow at a low (1 bubble/second) rate throughout the experiment.

The data thus obtained consisted of a series usually of 10-20 loads to rupture.

The inherent limitations of the apparatus and experimental method preclude the assignment of any significance to a single load reading. Thus, 10-20 readings taken in rapid succession a few mils apart are simply averaged and taken as an expression of the average compressive strength of the entire surface film at that time and temperature. Generally, the averaged points were then plotted as a function of time (see for example Figure 21) to obtain an indication of the rate-of-change of film strength with time under the various experimental conditions. Repeated experiments under identical conditions indicate that the overall shape, slopes, etc. of such plots are reproducible to within approximately 20 percent.

Experimental Results

Preliminary Experiments - Temperature Effects

Early experiments involved the study of the change of film compressive strength as a function of time and temperature using the relatively crude apparatus described in Reference (8). From these exploratory experiments, two kinds of data are of qualitative interest. Some of the data were analyzed in terms of distributions of the load required to rupture the film. Figures 2 and 3 show two such distributions; Figure 2 for pure E-105 ester and Figure 3 for a 5 (vol.) percent solution of TCP in E-105. While limitations in the apparatus made it impossible to determine average film strength at a given time interval, it is obvious that the TCP film becomes ulti-

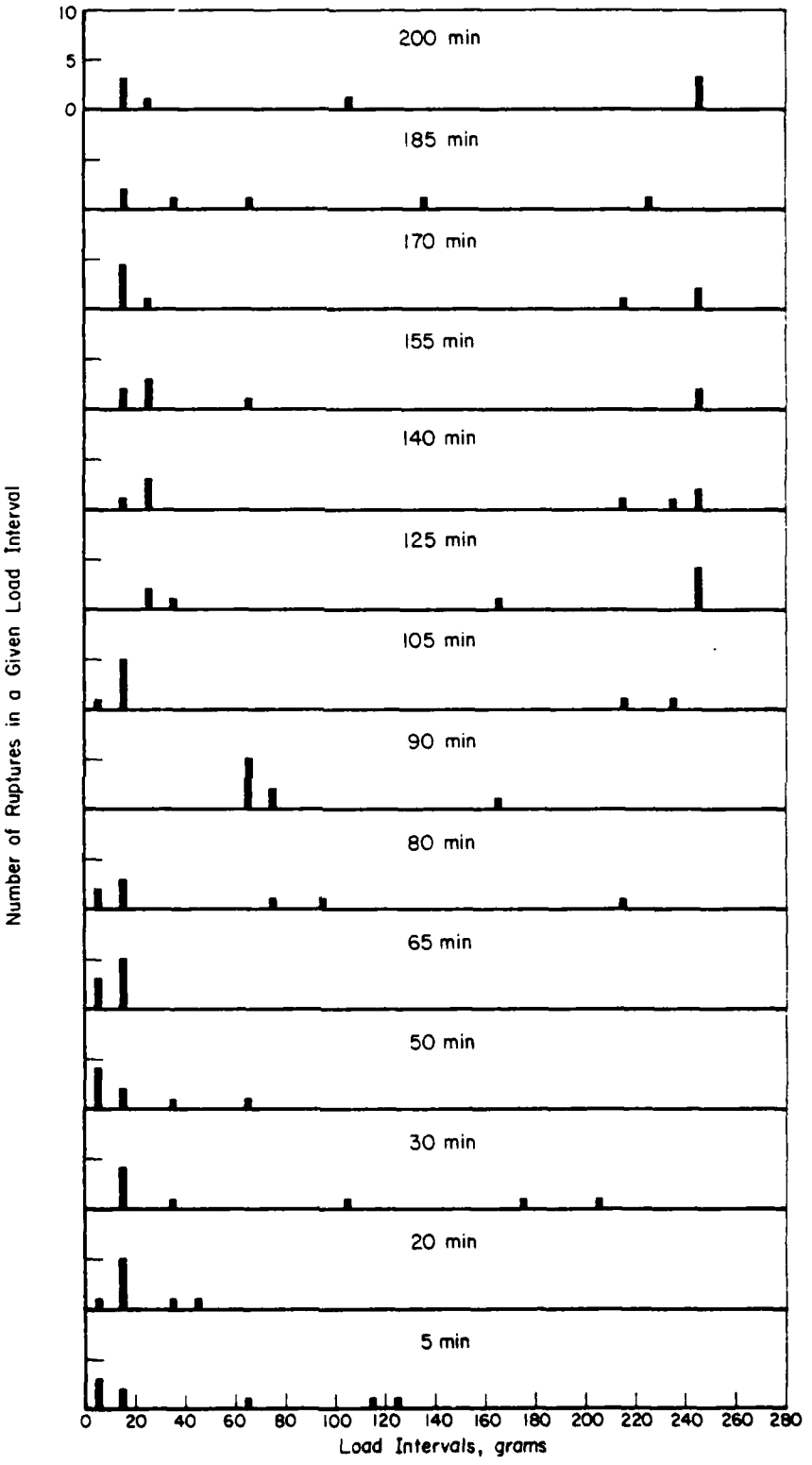

FIGURE 2. RUPTURE LOAD DISTRIBUTIONS AS A FUNCTION OF TIME FOR PURE E-105 ON ARMCO IRON AT 121 C

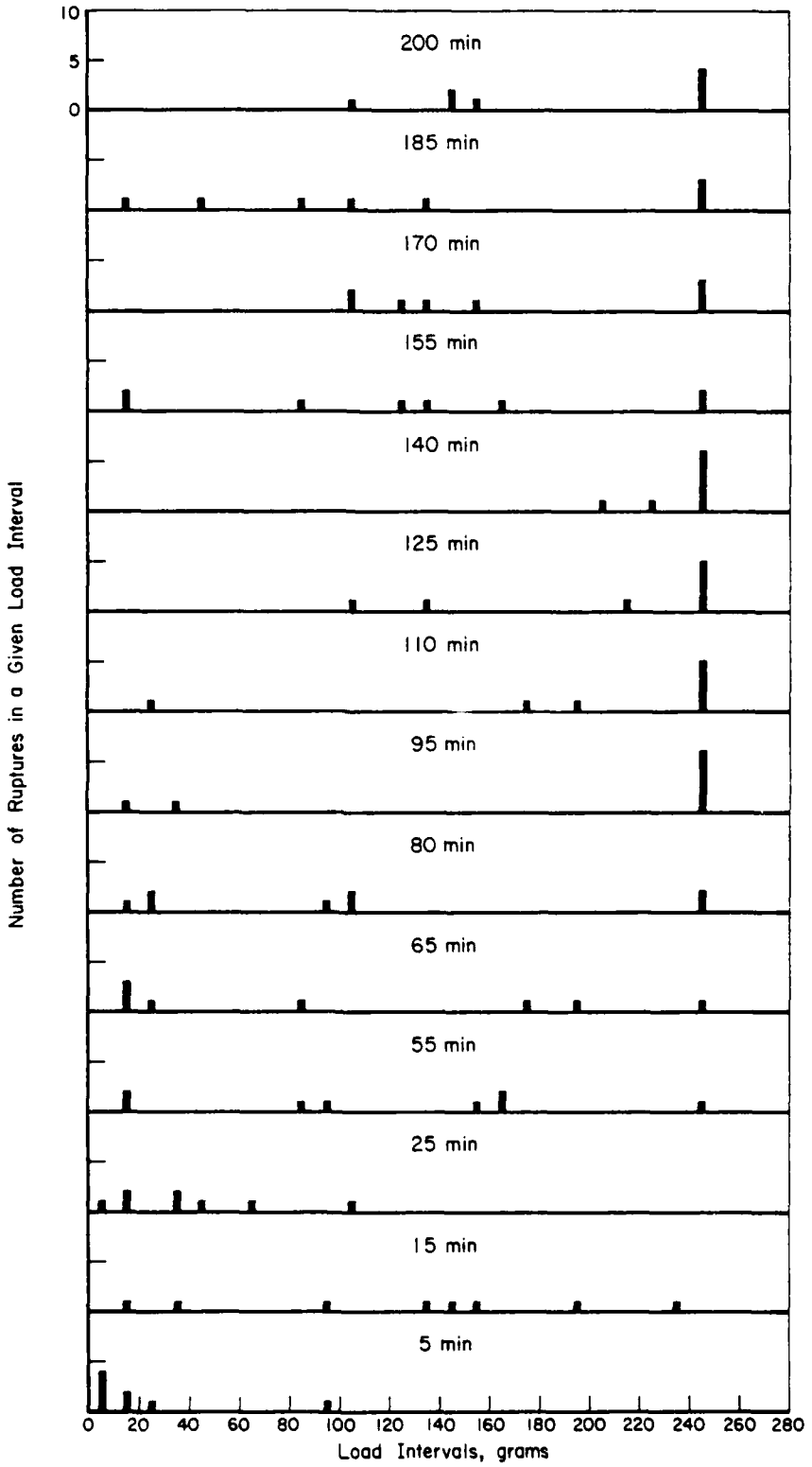

FIGURE 3. RUPTURE LOAD DISTRIBUTIONS AS A FUNCTION OF TIME FOR A 5 VOLUME PERCENT SOLUTION OF TCP in E-105 AT 121 C

mately much stronger than the ester film. This appears to be due, in part, to the distinct bimodality of the distribution of film strengths in the case of the films formed from pure ester. When the temperature is increased, the high strength "component" of the film disappears in the case of the ester film and does not in the case of a film formed with TCP/E-105. (Figures 4,5)

While these early data were not well-suited to rigorous slope (rate of change of load-to-rupture with time) determinations due to the limited load capacity and wide dead band of the apparatus, estimates of film strength increase rate were made for both pure E-105 and E-105 - 5 percent TCP solutions as a function of temperature. The data, summarized in Figure 6, indicate the onset of significant rates near 100-120 C.

After these experiments, the apparatus was modified by the addition of an automatic mechanical stylus lowering systems and increased load capacity.

Effects of Temperature and H_2O on Film Formation

Air Environment - Pure Ester. Figure 7 shows typical data from experiments carried out using pure E-105 on a freshly prepared ARMCO iron surface in bone dry air (dew point < -65 C) and in air nearly saturated with water vapor (rh ca. 85 percent). In this figure, the data are average film strength (load needed for film rupture) as a function of time for four different specimen, each at a different temperature level. The environment was bone dry air and the E-105 had been thoroughly dried with molecular sieve. Duplicate data are shown for the 95 C level in order to give an indication of the reproducibility of the data from specimen to specimen. From the limited number of experiments carried out on the pure ester, there appears to be a relationship between both the rate of formation and the strength of the film and the presence or absence of water.

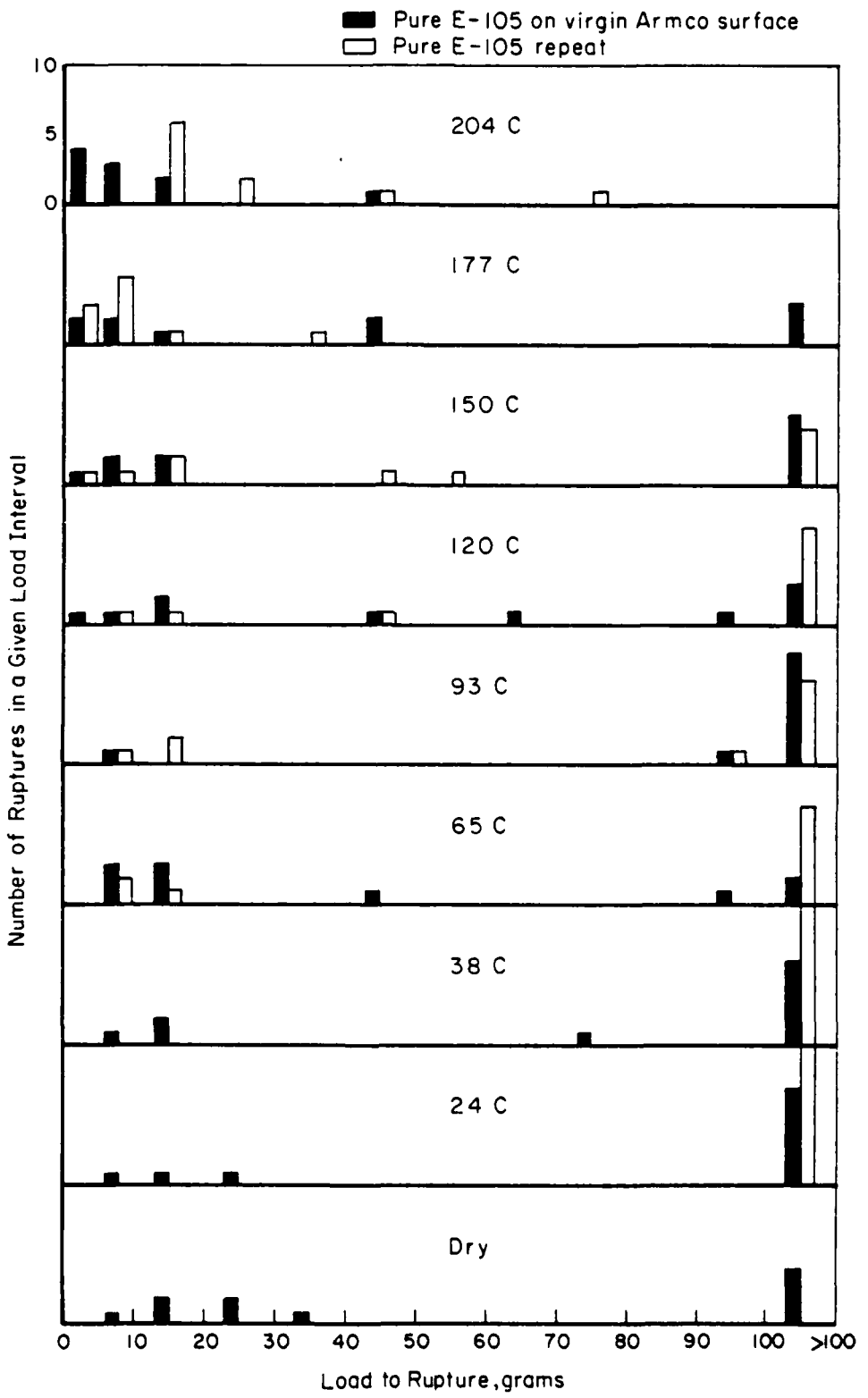

FIGURE 4. DISTRIBUTION OF LOADS-TO-RUPTURE FOR FILMS FORMED FROM PURE E-105 ON ARMCO IRON AS A FUNCTION OF TEMPERATURE

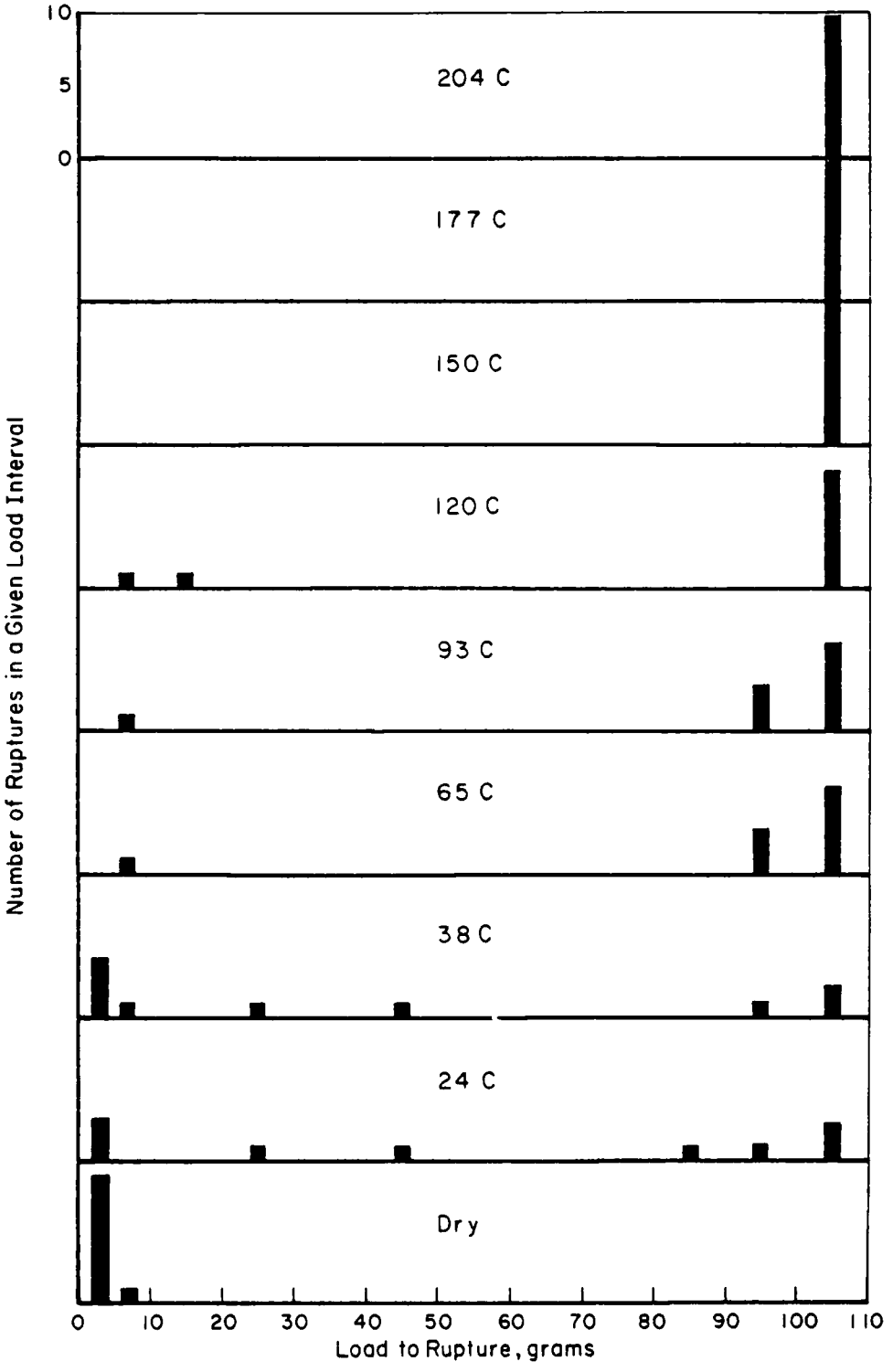

FIGURE 5. DISTRIBUTION OF LOADS-TO-RUPTURE FOR FILMS FORMED FROM E-105 CONTAINING 5 VOLUME PERCENT TCP ON ARMCO IRON AS A FUNCTION OF TEMPERATURE

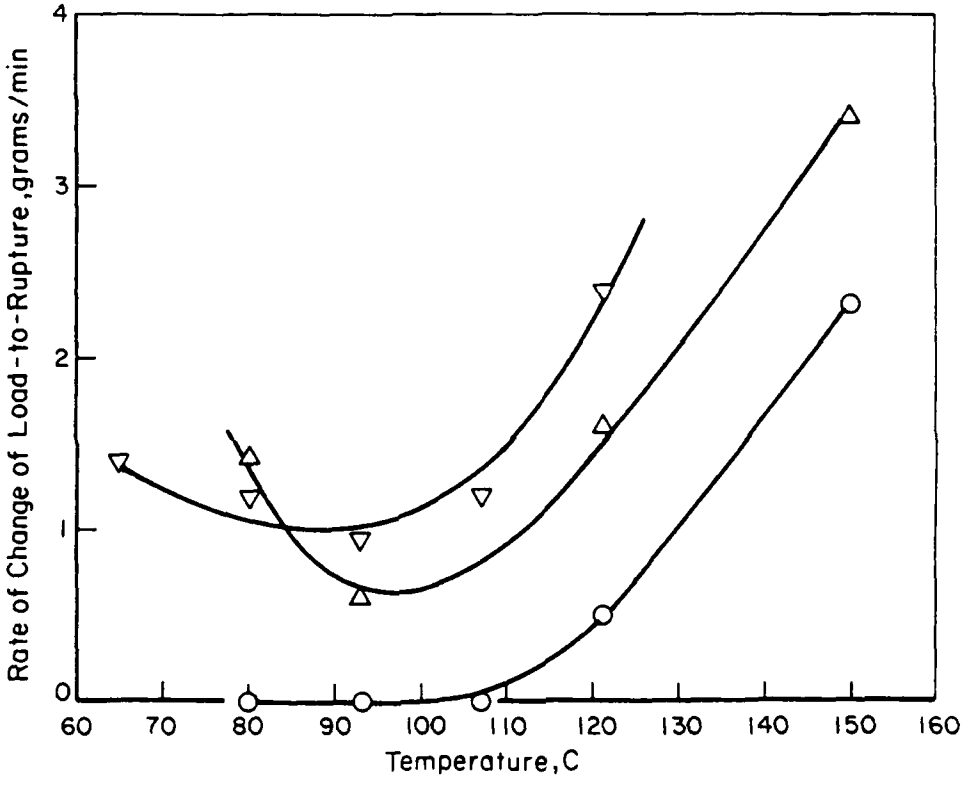

FIGURE 6. RATE OF CHANGE OF THE LOAD-TO-RUPTURE AS A FUNCTION OF TEMPERATURE FOR FILMS FORMED FROM PURE E-105 (CIRCLES) AND A 5 VOLUME PERCENT SOLUTION OF TCP IN E-105 (TRIANGLES)

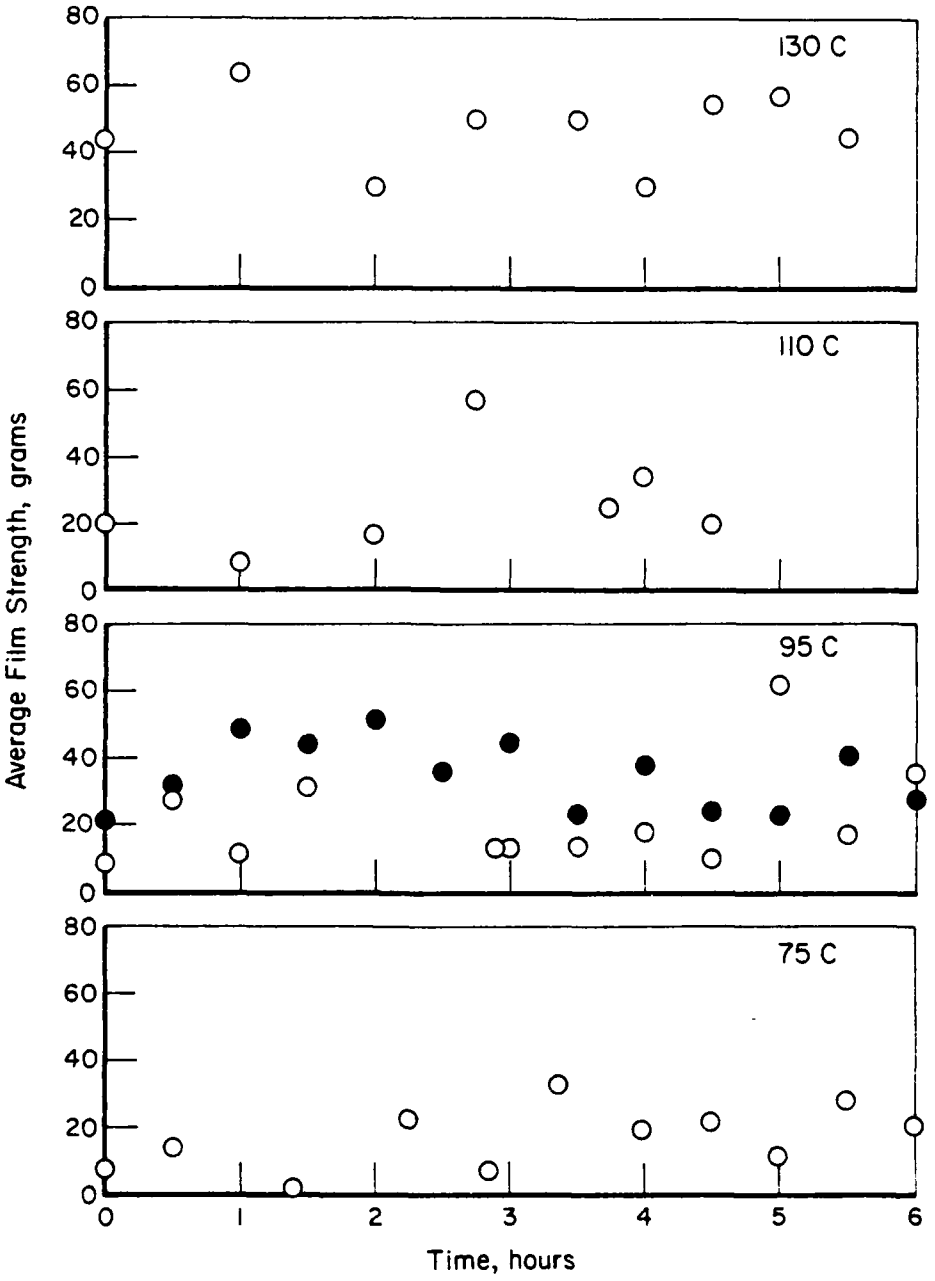

FIGURE 7. MEAN FILM RUPTURE STRENGTHS PROVIDED BY PURE E-105 FLUID ON ARMCO IRON IN "BONE DRY" AIR (Each Data Point Represents the Mean Value for 20 Determinations)

Figure 8 shows the average equilibrium strength of films formed from pure E-105 as a function of substrate temperature. In the absence of water, the films seem to increase in strength with increasing temperature, while in the presence of water, a minimum in strength is observed at approximately 80 to 100 C. It should be pointed out, however, that the experimental conditions - reactants in contact, with ample opportunity for continuing reaction as the isothermal measurements are taken - do not allow for the differentiation of kinetic effects and inherent film properties. Such differentiation would require the establishment of an equilibrium film, followed by removal of the reactants - E-105, air, and H_2O - prior to the mechanical characterization of the film at various temperature levels.

Figures 9 and 10 show the average film strength as a function of time for three temperature levels, in air, for solutions of 5 (vol) % TCP in E-105 with and without water. (Each temperature and environment is represented by a separate experiment and iron substrate.) A slope, representing a rate of increase of film compressive strength was estimated from each of the curves. In the case of the 130 C wet data, the compressive strength increased rapidly at temperature levels above 110 C and the slope was estimated from the heat-up curve (not shown). The solid line shown on that graph is from that heat-up curve. If the various slops (rates) are plotted as a function of substrate temperature, two curves reflecting the relative rates of formation under dry and "wet" conditions are obtained as shown in Figure 11. Below temperatures of the order of 100 C, water appears to have a definite retarding effect on the rate of formation of compressively strong boundary films. Above this temperature range, the presence of water is either beneficial or of little consequence. Additional experiments, in both air and argon, do not eliminate this ambiguity.

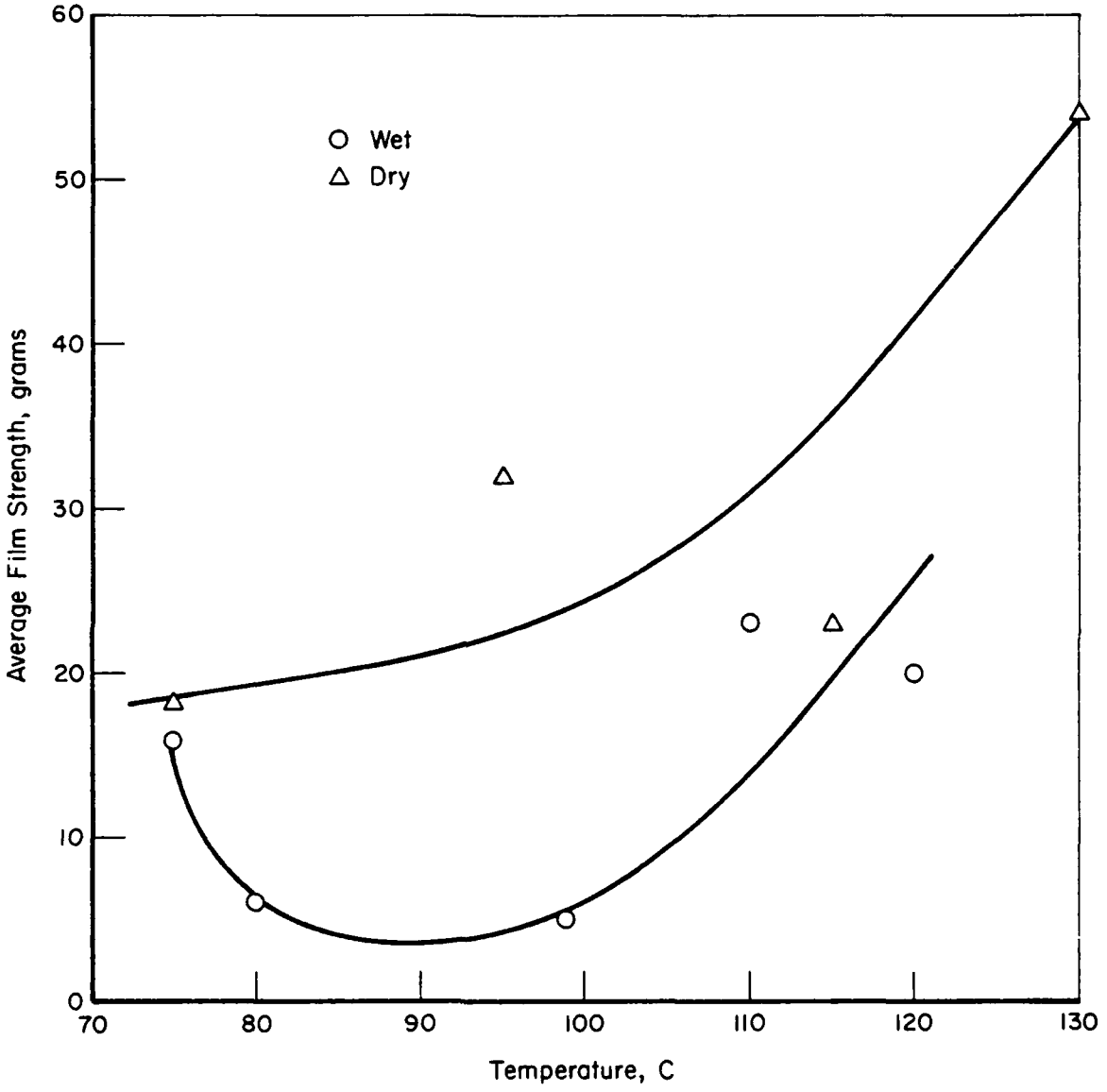

FIGURE 8. MEAN FILM RUPTURE STRENGTHS IN WET VERSUS DRY AIR ENVIRONMENTS FOR PURE E-105 FLUID ON ARMCO IRON (Each Data Point Represents the Mean Value for 20 Determinations.)

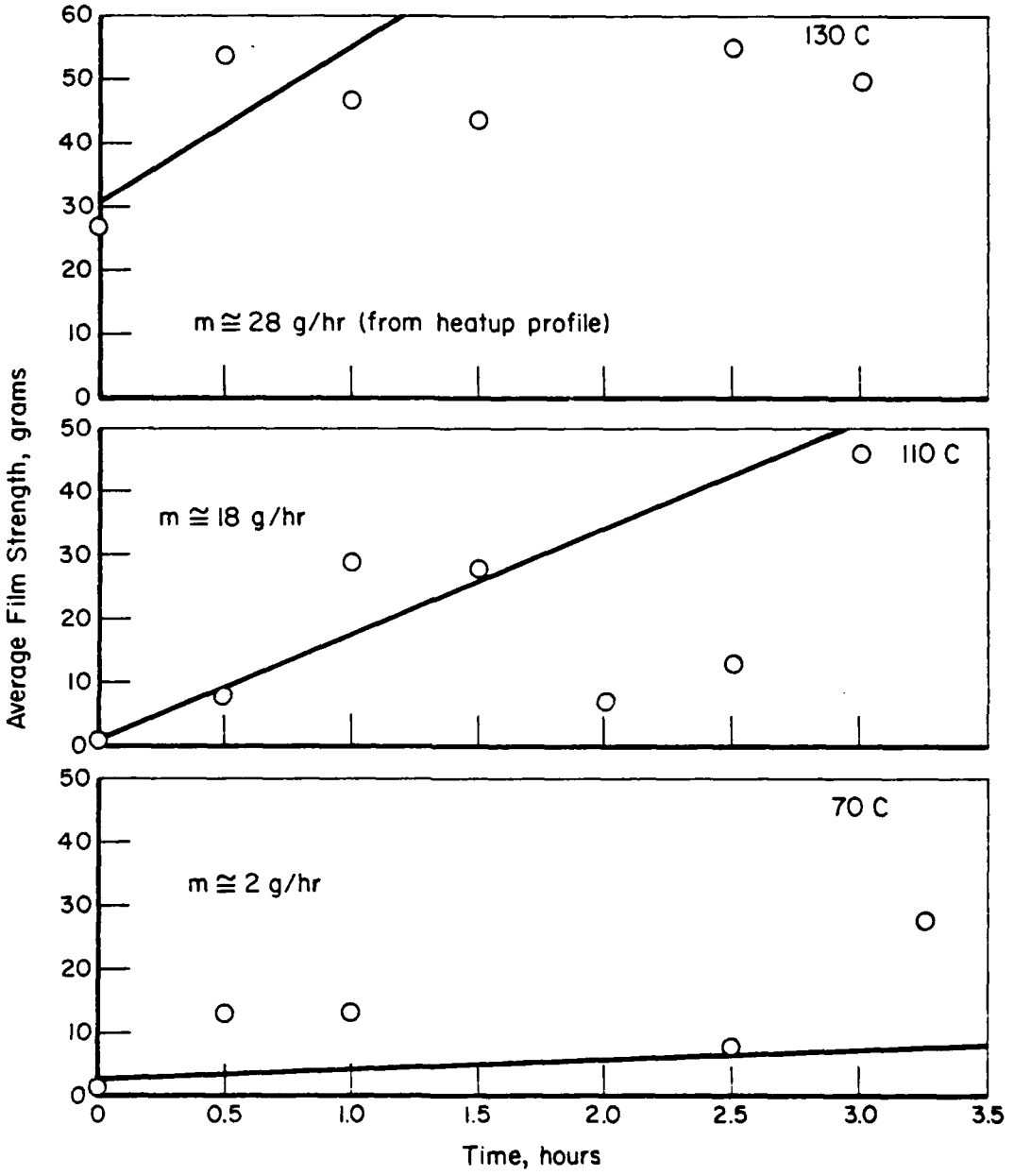

FIGURE 9. RATES OF INCREASE (m) IN FILM RUPTURE STRENGTHS FOR E-105 + 5 PERCENT TCP FLUID ON ARMCO IRON IN WET AIR ENVIRONMENTS

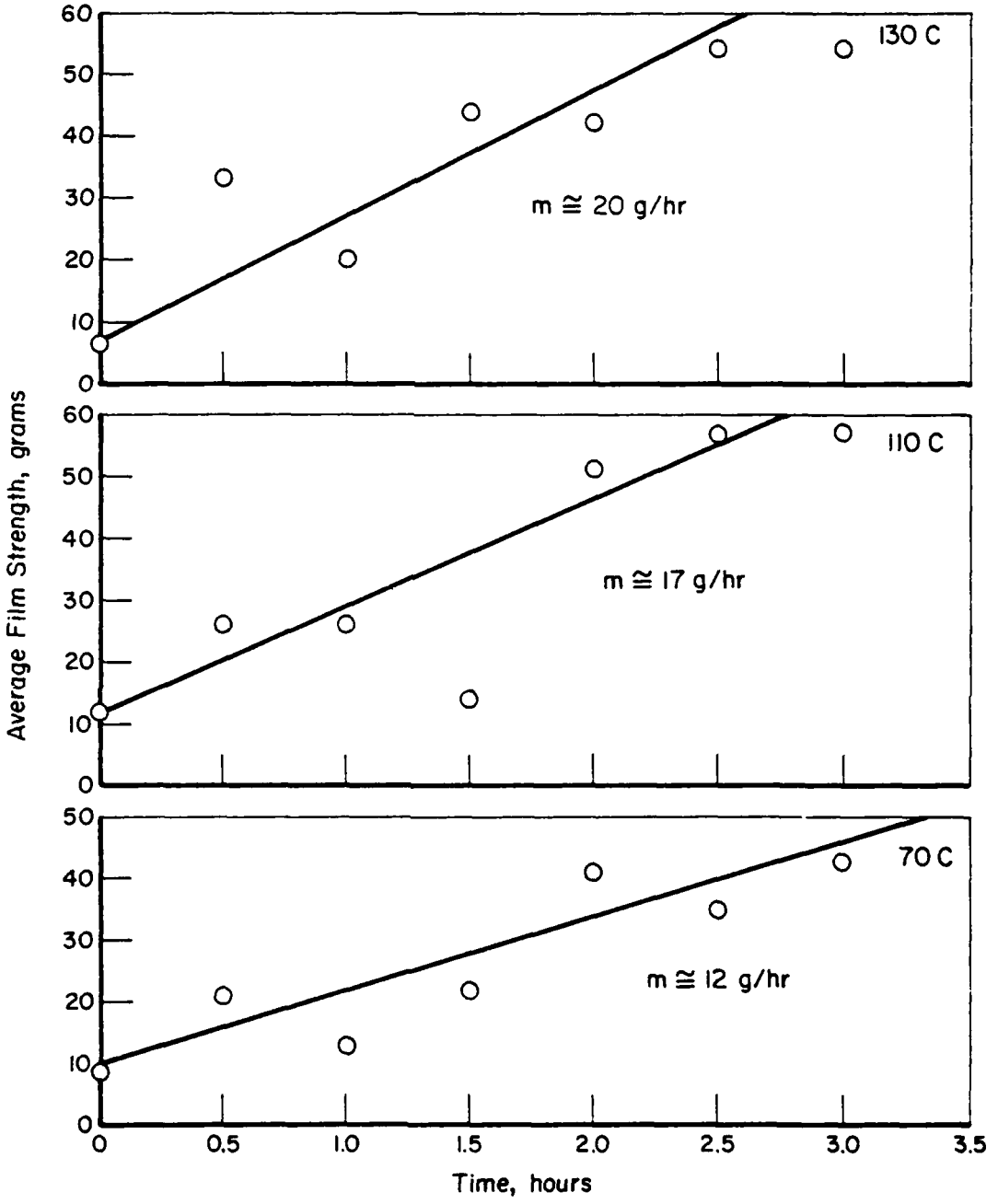

FIGURE 10. RATES OF INCREASED (m) IN FILM RUPTURE STRENGTHS FOR E-105 + 5 PERCENT TCP FLUID ON ARMCO (Run in Bone-Dry Air)

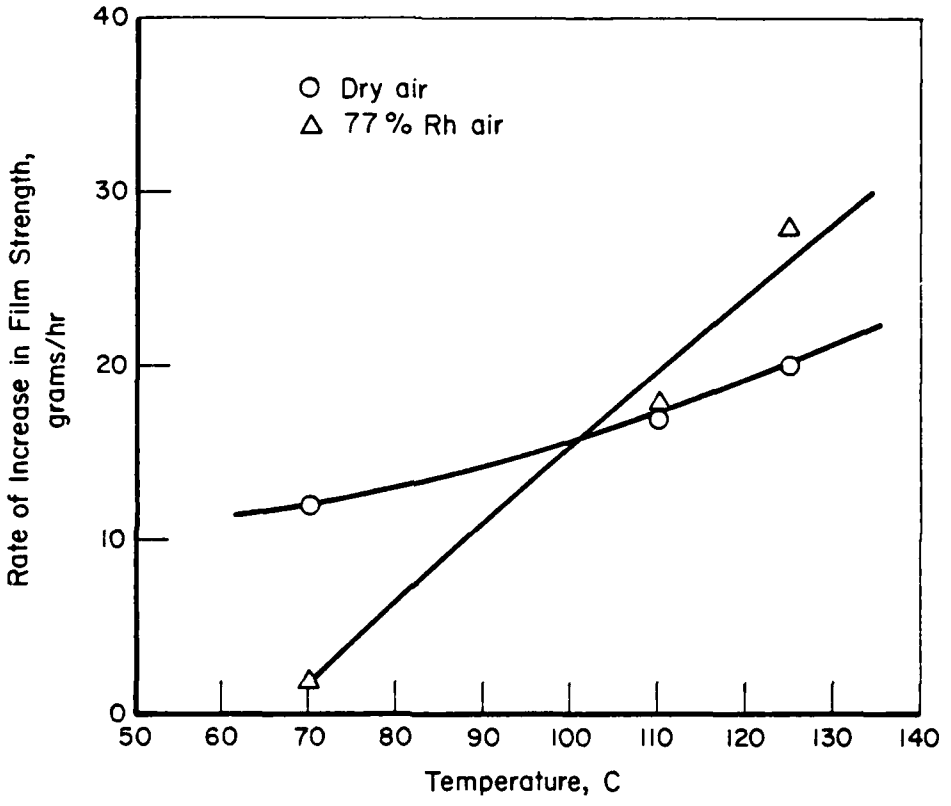

FIGURE 11. SURFACE FILM FORMATION RATES COMPARED FOR WET AND DRY AIR ENVIRONMENTS (E-105 + 5 PERCENT FLUID ON ARMCO IRON)

Argon Environment - E105-TCP Solutions. Experiments carried out in an atmosphere of pure argon - wet and dry - offer a dramatic contrast to those carried out in air. Figure 12 illustrates the behavior of E-105 + TCP films in dry argon in terms of the average film strength as a function of time at several temperature levels. Temperatures up to 300 C and reaction times of nearly 8 hours produced average strength films that were 2 to 10 times weaker than films formed in the presence of air. Figure 13 shows data comparing an experiment carried out in dry argon with one carried out in argon with a relative humidity of approximately 85 percent. Both experiments were carried out under isothermal conditions at 110 C. The presence of H_2O appears to influence the equilibrium film strength but not the rate at which the strength, such as it is, develops. The film formed in dry conditions is slightly stronger than that formed under wet conditions. Figures 14 and 15 show the data depicted in Figure 9 superimposed upon the average film strength as a function of time for Figure 9 superimposed upon the average film strength as a function of time for two experiments carried out in air. The role of water, at temperatures above its boiling point, remains unclear. The differences between wet and dry in the various experiments, depicted in Figures 11, 13, 14, and 15 are probably within experimental error.

Several experiments were carried out on a film formed from E-105 + 5 percent TCP in dry argon. This film was formed at 110 C and was subjected to temperature exposures as high as 150 C in the dry argon environment. Throughout these experiments, the average strength remained relatively low - 3 to 8 grams. After several hours of thermal cycling - which indicated no temperature dependency of film strength within experimental error - argon saturated with water vapor and E-105 liquid saturated with H_2O were admitted in such a way as to preclude the introduction of O_2 and average film strength measurements made as a function of time and temperature. Figure 16

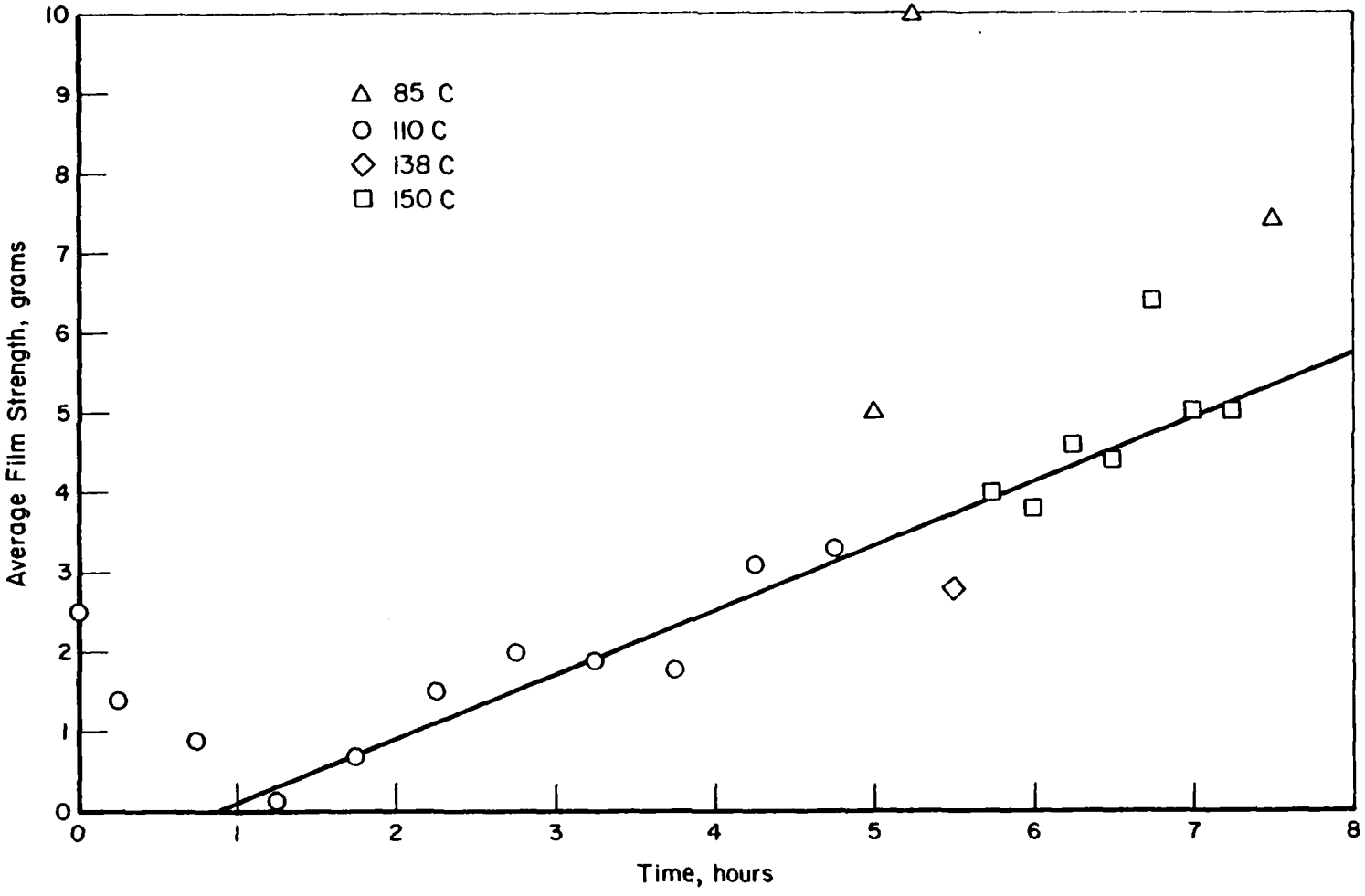

FIGURE 12. MEAN AVERAGE FILM RUPTURE STRENGTHS FOR E-105 + 5 PERCENT TCP FLUID ON ARMCO IRON IN DRY ARGON

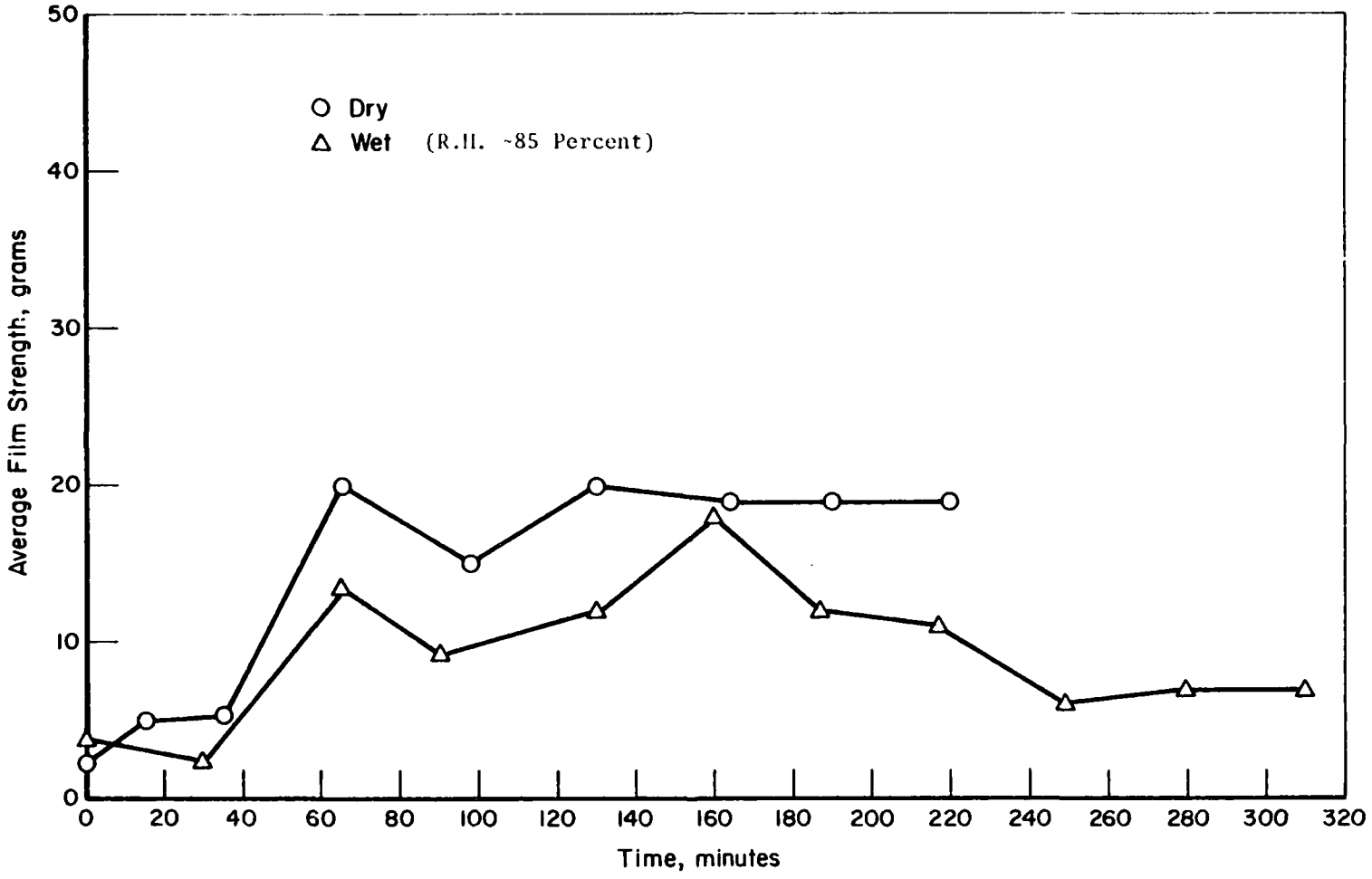

FIGURE 13. MEAN FILM RUPTURE STRENGTHS PROVIDED BY E-105 + 5 PERCENT TCP FLUID ON ARMCO IRON IN DRY AND IN WET ARGON AT A CONSTANT TEMPERATURE OF 110 C

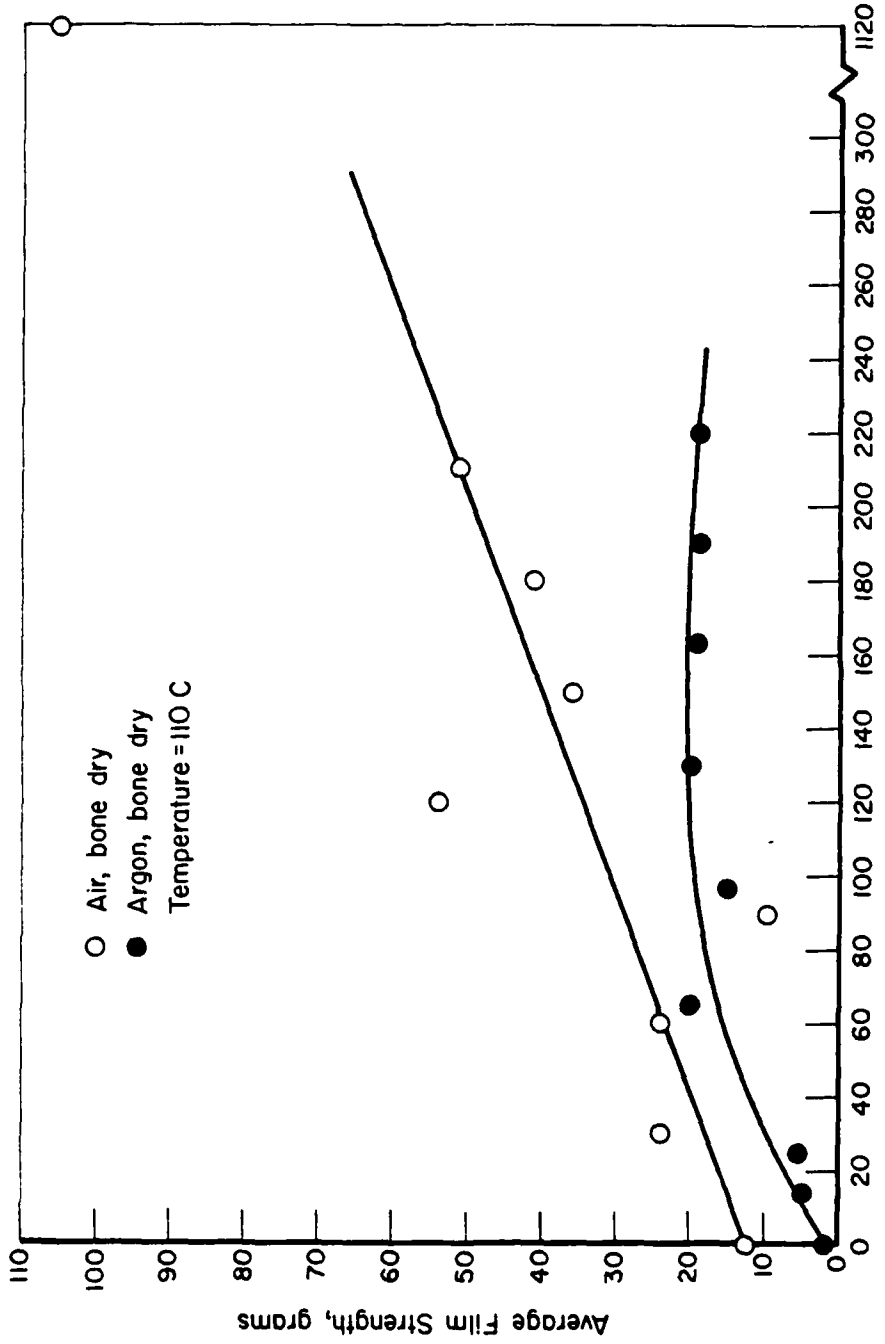

FIGURE 14. MEAN FILM RUPTURE STRENGTHS FOR DRY AIR AND DRY ARGON COMPARED (E-105 + 5 PERCENT TCP LIQUID PHASE) AT A CONSTANT TEMPERATURE OF 110 C

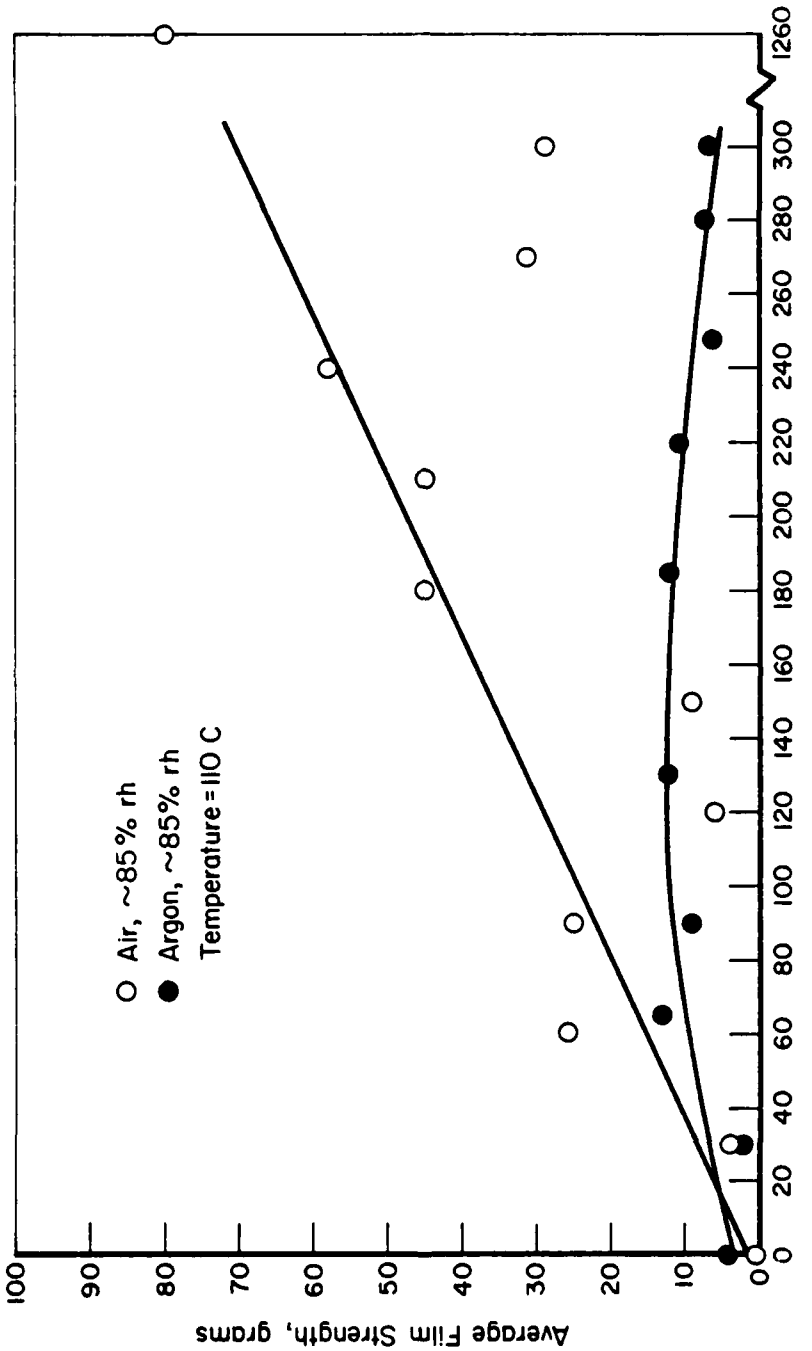

FIGURE 15. MEAN FILM RUPTURE STRENGTHS FOR WET AIR AND WET ARGON COMPARED (E-105 + 5 PERCENT TCP LIQUID PHASE) AT A CONSTANT TEMPERATURE OF 110 C

shows the average film strength as a function of time from the introduction of water. Each data point on the graph represents the average of 21 individual, successive measurements of the load required to rupture the film. (The high average at t = 0 is probably anomalous, the average being dominated by two readings of an unusually high level. This apparent drop in strength with the introduction of water should not be construed as a water effect. The data point (not shown) just prior to that at t = 0 was 2.5 grams - a value consistent with the post-H_2O strength levels.) After some 6 hours of exposure to humid argon and H_2O-saturated E-105, the average film strength had not increased more than 2 grams over a wide temperture range. At this point, laboratory air was admitted (45 percent relative humidity). After an induction period of approximately 15 minutes, possibly reflecting the diffusion of O_2 through the oil film, the average film strength began to increase dramatically (right-hand portion of the curve in Figure 16).

In contrast to films formed in air, those formed in argon tend to be more uniform with respect to strength with extreme values for individual readings absent. For example, none of the bimodality observed in air-formed films is present. Readings of high- or low-compressive strength appear to occur in groups suggesting that the succession of measurements is traversing regions of high- and low-film strength and that the appearment scatter in the results is due to variation in the properties of the surface film and not necessarily to inherent experimental scatter. Figure 17 shows the rupture load values for a series of 36 readings, each approximately 10 mils apart, on a film formed in dry argon. Portions A, B, and C suggest areas of high (B, C) and low (A) strength on the surface.

Early experiments indicate that films formed in air show a wide variation in individual strength values at a given time and temperature. The distributions of values tend to fall into a bimodal distribution with low and high values and relatively few in between. Figure 18 shows the percent of values over 20 grams as a function of time for

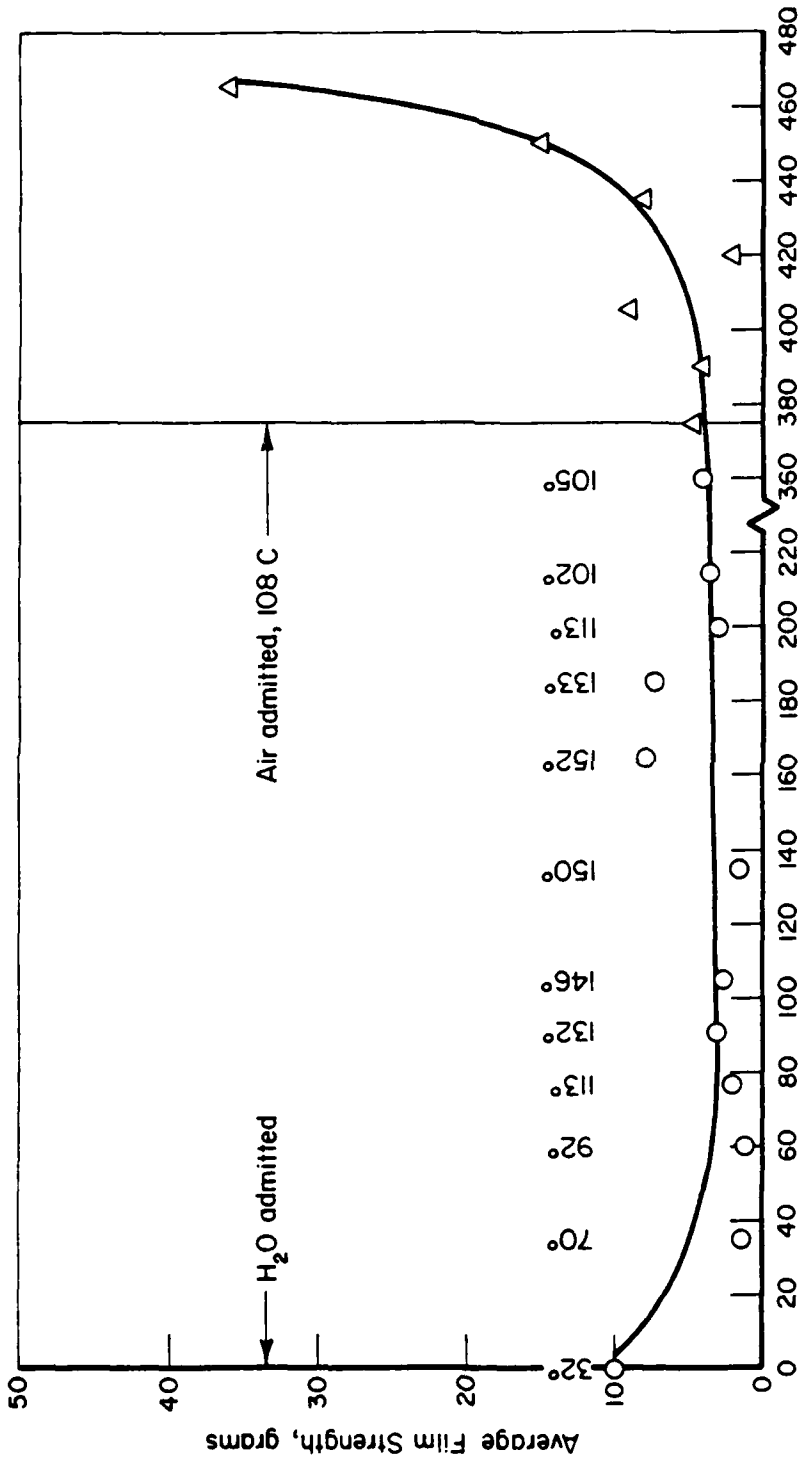

FIGURE 16. MEAN FILM RUPTURE STRENGTHS FOR E-105 WITH 5 PERCENT TCP ON ARMCO IRON BEGUN IN DRY ARGON

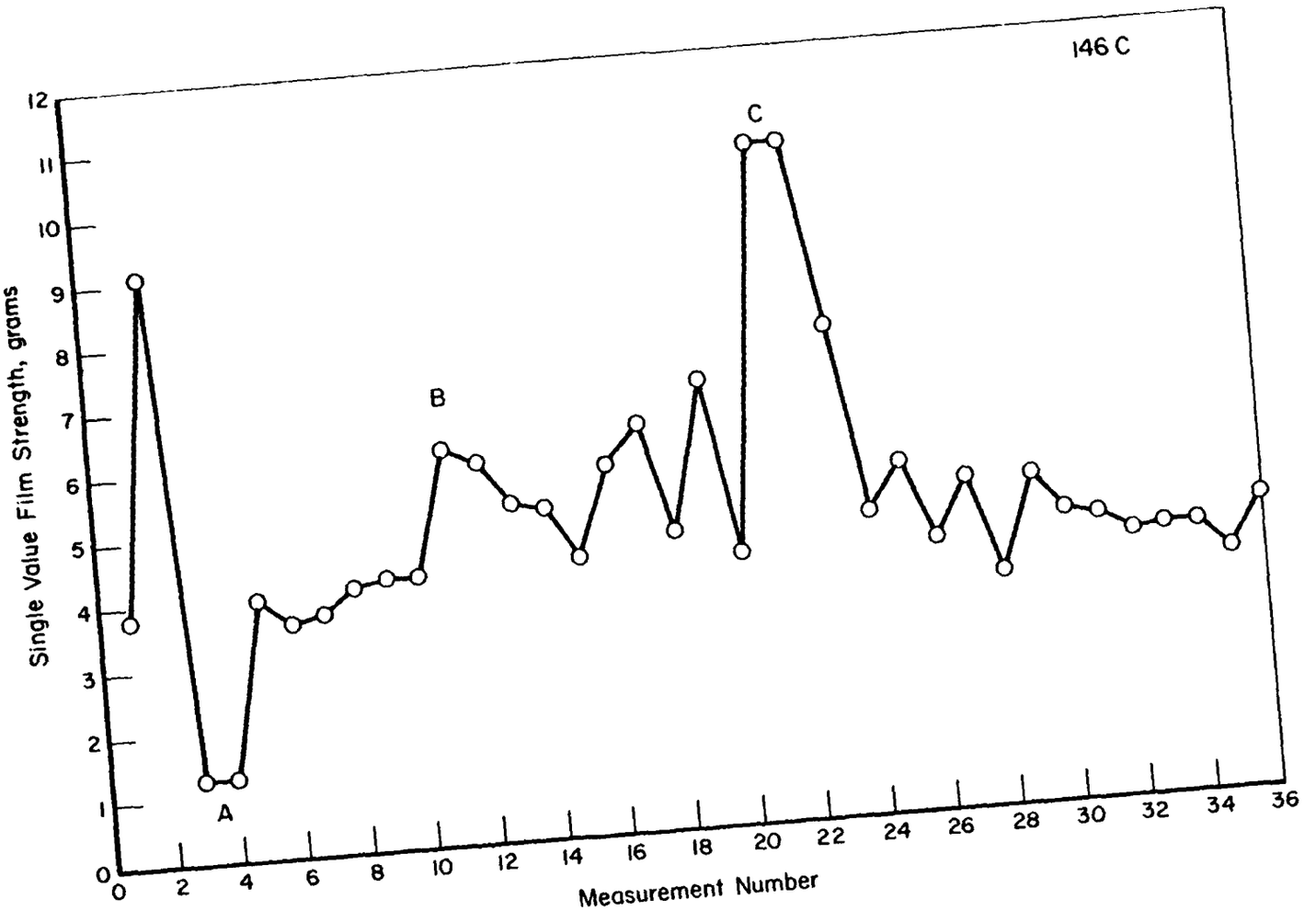

FIGURE 17. TYPICAL FILM RUPTURE STRENGTH VARIATION ACROSS SPECIMEN SURFACE FOR AN EXPERIMENT IN AN ARGON ENVIRONMENT

wet and dry air. The high-strength fraction tends to increase with time at approximately the same rate for both wet and dry conditions. Figure 19 shows the same treatment of the data for films formed in argon. There is virtually no high-strength component and no significant difference between wet and dry. Thus, it appears that the development of high-strength films depends upon a high-strength component that requires O_2 for its formation.

Effects of O_2 and TCP Concentration

Prior to these experiments, the apparatus was modified by the replacement of the mechanical stylus actuator to the pneumatic system described in the Apparatus Section. This increased the sensitivity and reproducibility of the apparatus. In addition, the temperature of reaction was increased from 110 C to 120 C in order to increase the rate of the reactions and thus decrease reaction time.

Figures 20 and 21 show the average load required to rupture a film plotted as a function of time at temperature for experiments carried out at 110 and 120 C, respectively. Note that, in both cases, the curves appear to be the resultant sum of two linear functions, as shown in Figure 20. The data in Figure 20 were analyzed by a least squares analysis both as 2 linear functions. Hence, it is assumed for the present time that the data for the fit as an exponential was 0.86 as compared to 0.55 and 0.40 for the two linear functions. Hence, we are assuming for the moment that the data for the reaction in laboratory air are best represented by the sum of two linear functions having slopes of 5 g/hr and 24 g/hr. The data in Figure 21 were taken at 120 C and this seemingly innocuous change in reaction temperature (made to shorten experiment times) has resulted in an unexplainable decrease in the higher slope of from 24 to 10 g/hr. The lower slope remains essentially unchanged at 5 g/hr.

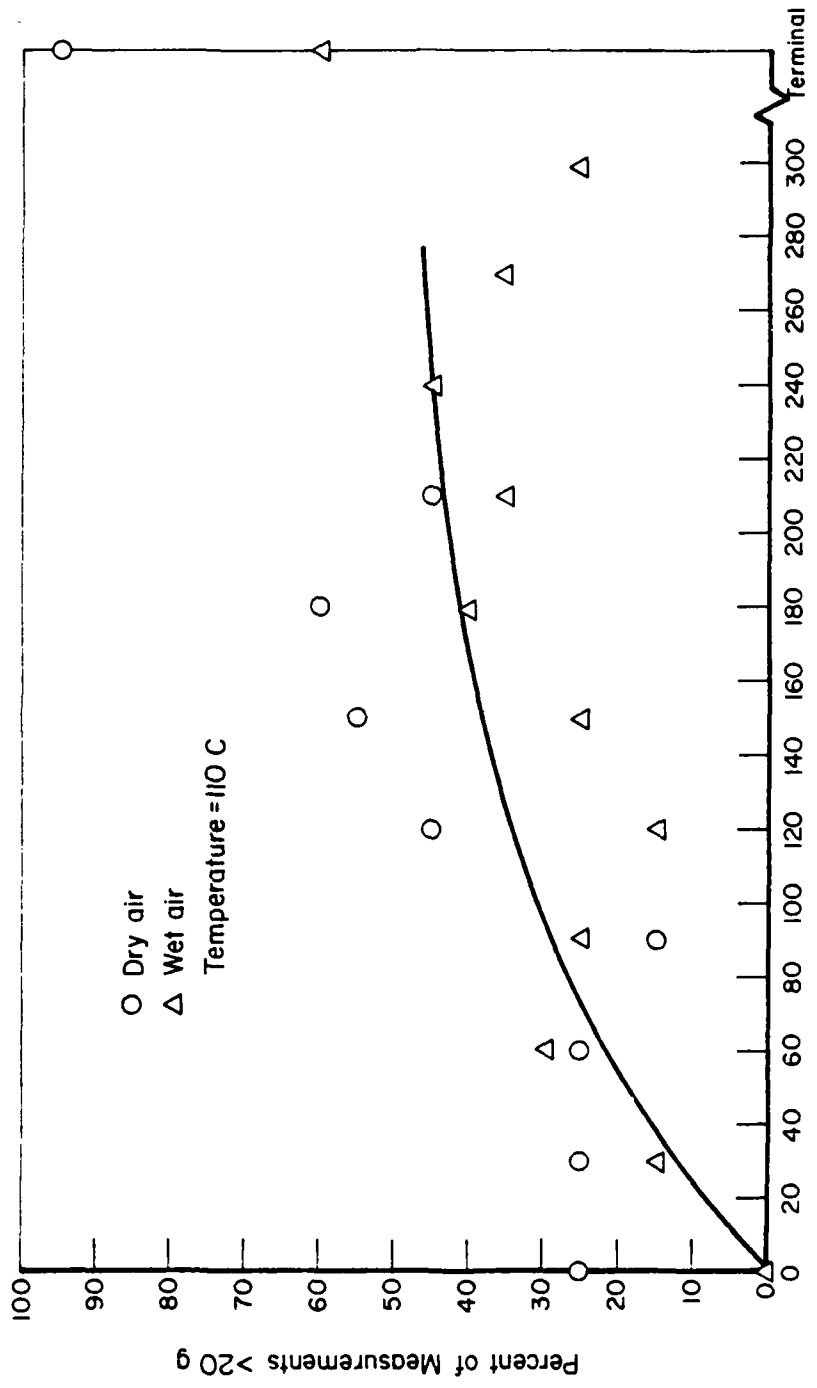

FIGURE 18. RATE OF INCREASE IN PERCENTAGE OF HIGH-STRENGTH POINTS FOR E-105 + 5 PERCENT TCP FILMS IN AIR ENVIRONMENTS (Compare with Figure 15.)

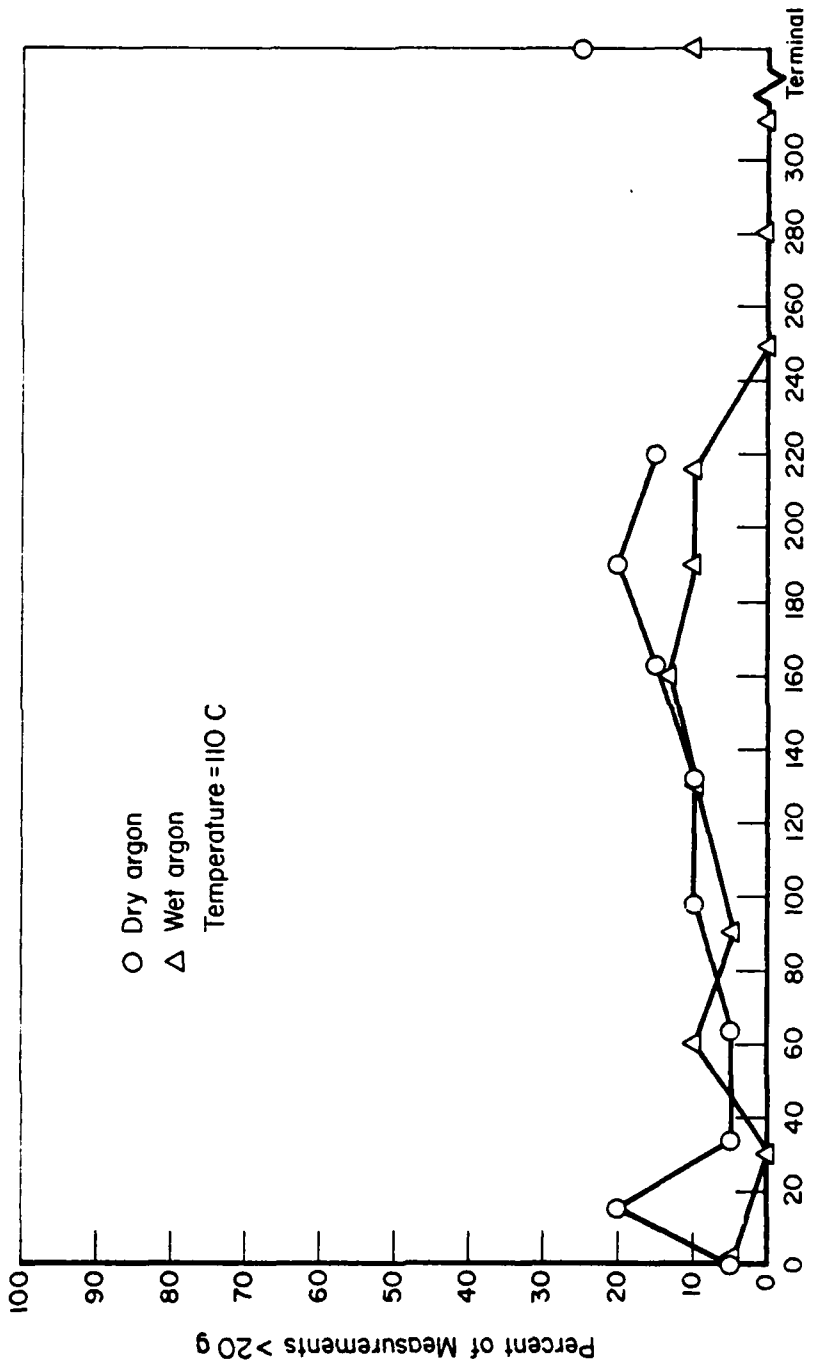

FIGURE 19. UNIFORMITY IN THE PROPORTION OF HIGH-STRENGTH POINTS FOR E-105 + 5 PERCENT TCP FILMS IN ARGON ENVIRONMENTS (Compare with Figure 14.)

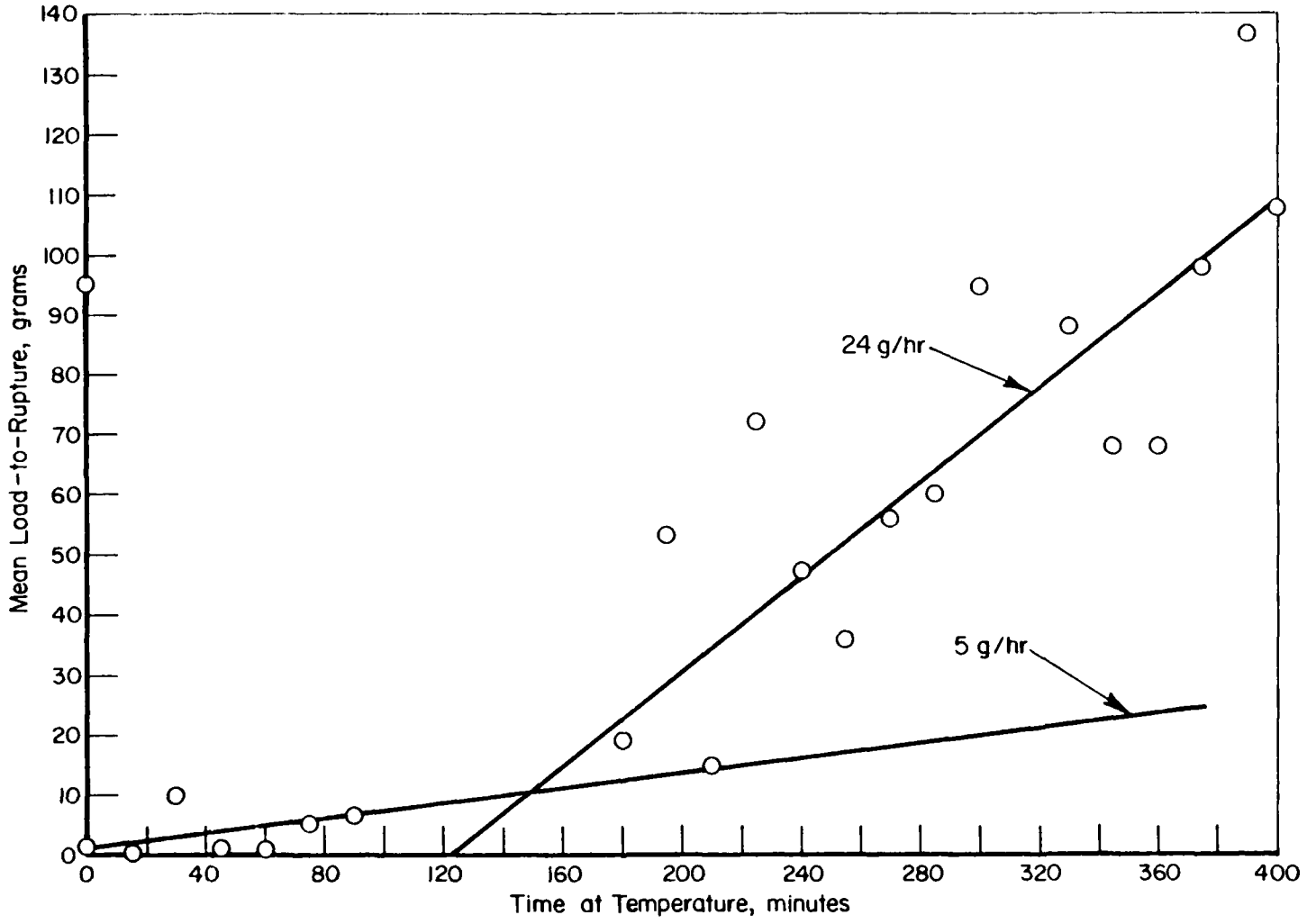

FIGURE 20. MEAN LOAD REQUIRED FOR FILM RUPTURE AS A FUNCTION OF TIME FOR A FILM FORMED FROM 5 PERCENT TCP (WT.) IN E-105 IN AN ATMOSPHERE OF LABORATORY AIR (RELATIVE HUMIDITY ≅ 65 PERCENT). THE TEMPERATURE OF THE ARMCO IRON SUBSTRATE WAS 110 C.

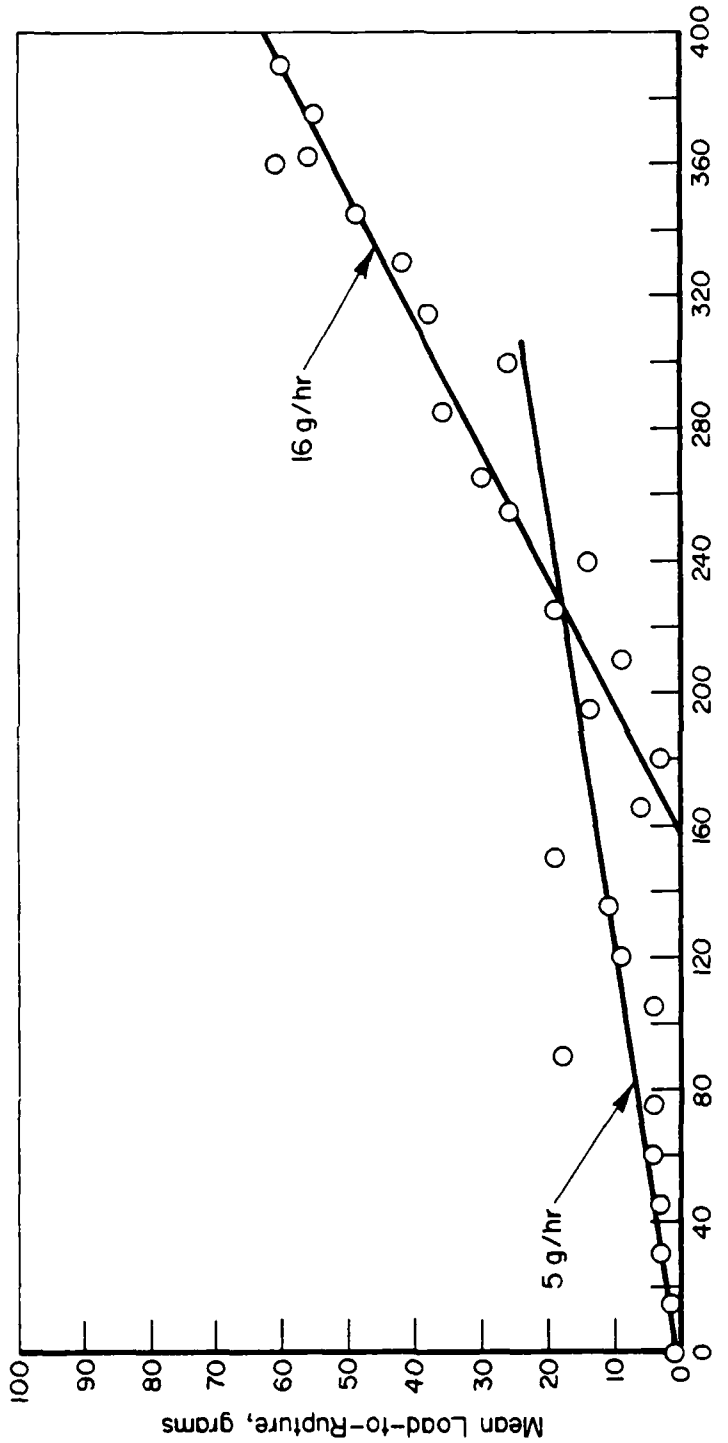

FIGURE 21. MEAN LOAD REQUIRED FOR FILM RUPTURE AS A FUNCTION OF TIME FOR A FILM FORMED FROM 5 PERCENT (WT.) TCP IN E-105 IN AN ATMOSPHERE OF LABORATORY AIR (70 PERCENT RELATIVE HUMIDITY). THE TEMPERATURE OF THE ARMCO IRON SUBSTRATE WAS 120 C.

Besides temperature, the only ostensible difference between these experiment is relative humidity -- 65 percent in the case of the 110 C experiment and 70 percent in the case of the 120 C experiment. There may be subtle H_2O effects not obvious in the previous research associated with the effects of humidity on reaction rates. Additional work in this area is indicated.

By themselves, these curves cannot be interpreted in terms of the processes leading to the formation of compressively-strong boundary films. Thus, it is instructive to consider the same kind of data taken from experiments carried out in argon and argon-oxygen mixtures.

Table 1 shows slopes of plots of the average load required to rupture a film versus time for films formed in pure argon, 1 percent O_2 in argon, 5 percent O_2 in argon, and 20 percent O_2 in argon. The results are striking. As previously reported substantial films do not form in the absence of O_2. One surprising finding is the observation that 1 percent oxygen in argon behaved essentially as pure argon and that 5 percent and 20 percent (the "argon-analogue" of dry air) are essentially identical. Thus, the data suggest that while O_2 is critical to the formation of strong films, there exists a "threshold effect" wherein small concentrations of O_2 (between 1 and 5 percent) play no significant role in the formation of films. Further, it was observed that air (essentially 20 percent O_2 in N_2) produces a complex curve that may be the result of 2 linear processes, while O_2 in Ar produces an essentially simple linear relationship, the slope of which is very similar to that of the high slope component of the curve from the air-formed film.

After 270 minutes of reaction in pure Ar at 120 C opening the system to lab air (75 percent RH) yielded the results shown in Figure 22. The film strength increased quickly to a value of about 27 g and then gradually increased with a slope of 11 g/hr -- a figure quite similar to the 10-15 g/hr slope associated with the final por-

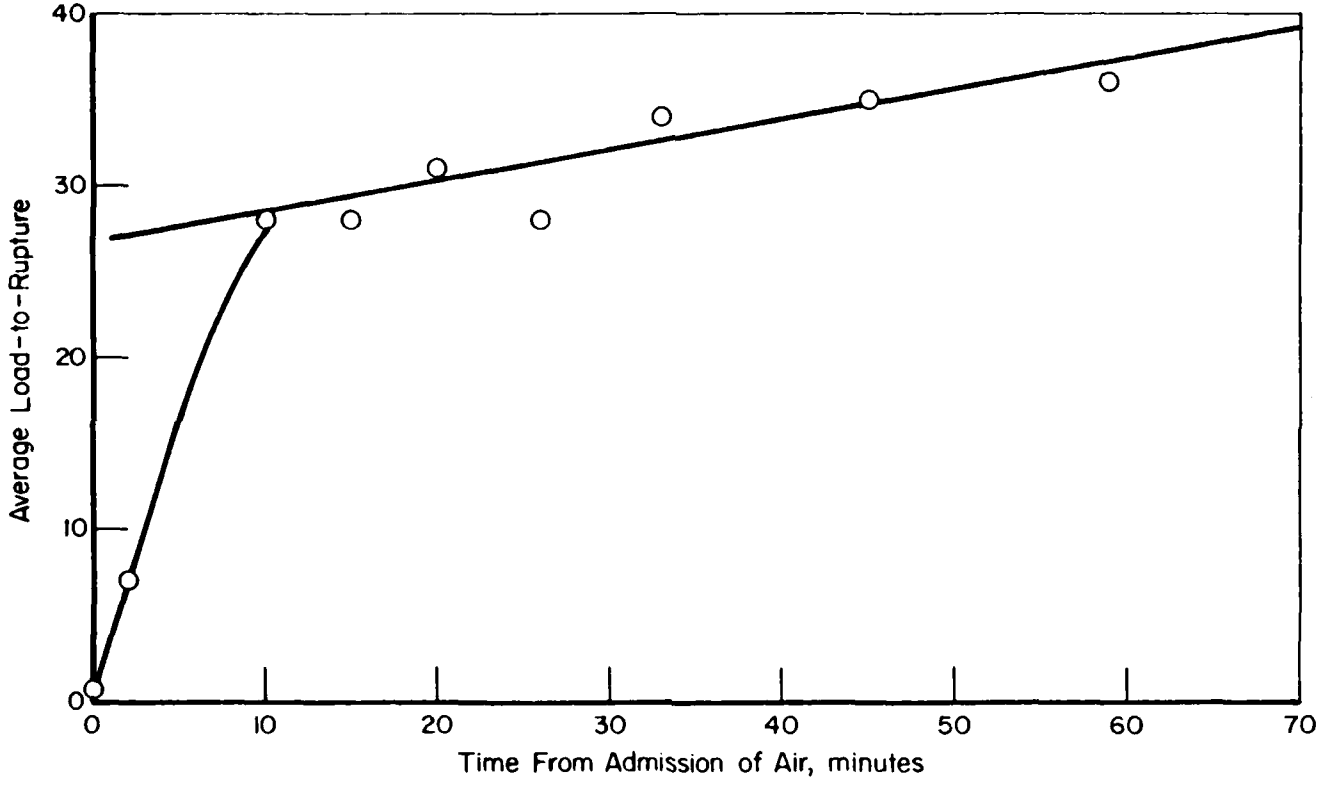

FIGURE 22. THE EFFECTS OF THE INTRODUCTION OF AIR (RELATIVE HUMIDITY = 75 PERCENT ON A FILM FORMED FROM 5 PERCENT (WT.) TCP IN E-105 IN DRY ARGON AT 120 C. THE ARMCO IRON SUBSTRATE TEMPERATURE WAS HELD AT A CONSTANT 120 C THROUGHOUT.

tion of the curves resulting from reaction in laboratory air, and to curves obtained in O_2/Ar mixtures.

TABLE 1. THE EFFECTS OF OXYGEN CONCENTRATION ON THE SLOPES OF COMPRESSIVE STRENGTH VERSUS TIME CURVES FOR 5% TCP IN E-105 REACTED AT 120 C

O_2 Concentration in Pure Dry Argon	Slope g/hour
0	0
1	2×10^{-3}
5	13
20	15

Effects of TCP Concentration

The results of a typical experiment involving variations in the concentration of TCP are shown in Figure 23. These data are for an experiment with 1% TCP in E-105 at 120 C in 20% O_2/Ar. This shape is characteristic and resembles that obtained in air. For concentration ranges from 1% (0.03 M) TCP to 5% (0.14 M) TCP in E-105, the concentration change results in a change in the time required for the onset of the growth of film strength (induction period) only. The rate at which the film strength develops following induction appears to be more-or-less independent of TCP concentration (Table 2).

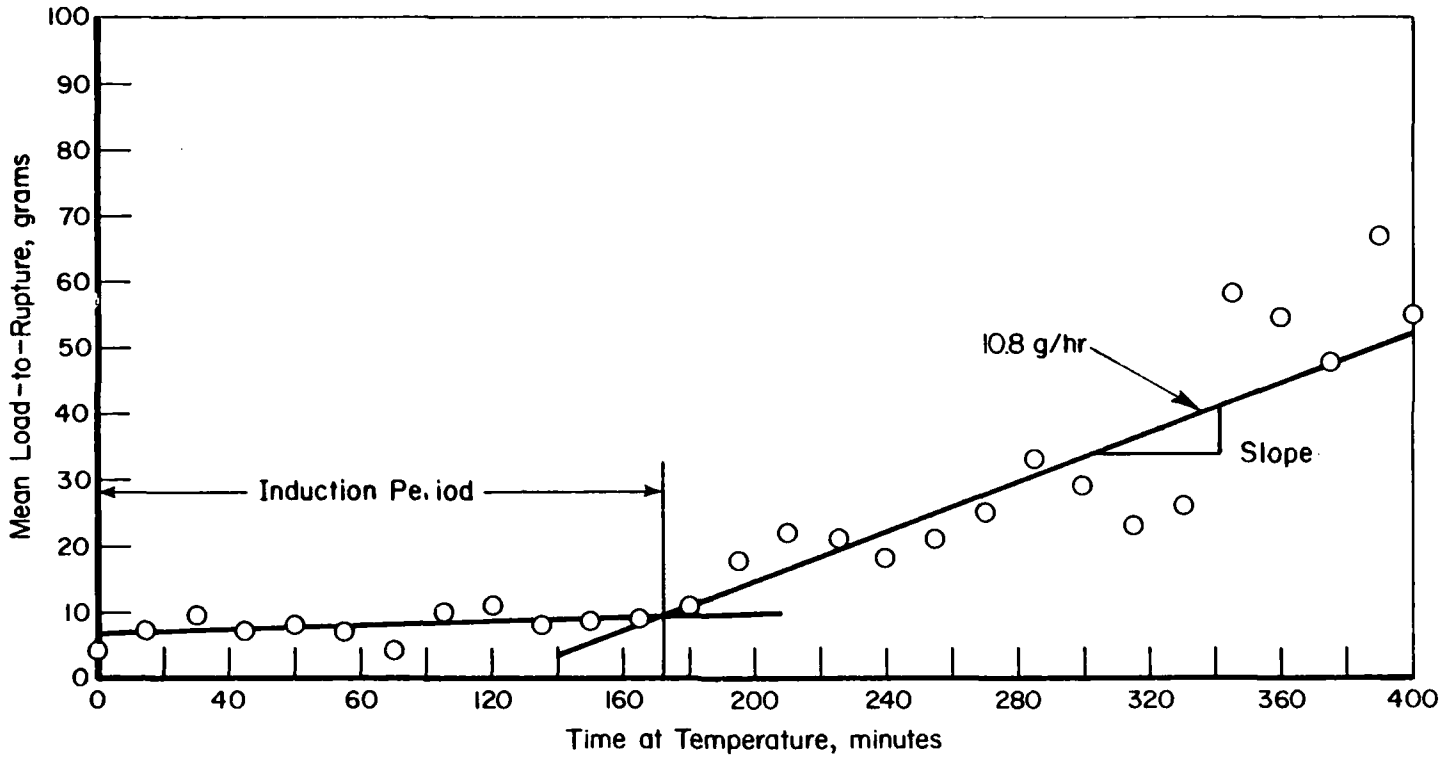

FIGURE 23. MEAN LOAD REQUIRED TO RUPTURE THE BOUNDARY FILM AS A FUNCTION OF TIME FOR A FILM FORMED FROM A SOLUTION OF 1 PERCENT (WT.) TCP IN E-105 IN A DRY ATMOSPHERE OF 20 PERCENT O_2 IN AIR. THE TEMPERATURE OF THE ARMCO IRON SUBSTRATE WAS 120 C.

TABLE 2. THE EFFECTS OF THE CONCENTRATION OF TCP IN E-105 ON THE RATE OF INCREASE OF COMPRESSIVE STRENGTH OF FILMS ON ARMCO IRON (The reaction temperature was 120 C, the atmosphere dry 20 percent O_2 in argon.)

Volume % TCP	Molarity TCP	Slope in g/hr	Induction Period minutes
0	0	0	(no reaction)
1	.03	11	70
3	.09	14	100
5	.14	15	15
50	1.4	10	75
100	2.8	15	240

In a similar system - TCP in octadecane at 248 C in air - Llopis and coworkers (9) report that film thickness (measured radiochemically) increases with increasing TCP concentration to approximately 0.12 molar. At this concentration, it levels off and becomes more-or-less independent of concentration. A minimal variation in rate is shown in this work as compared to the work of Llopis, et al. However, because of the reaction times involved in the latter work (2 hours), the induction effect could be strongly influencing the data at concentrations below 0.1 molar.

The research of Llopis shows an order-of-magnitude reduction in film thickness for experiments carried out in N_2 - a figure which compares quite favorably with the results of our experiments carried out in Argon. Thus, a cautious comparison can be made of film strength with film thickness for TCP films and suggests that there is a relationship between the two.

SEM Analyses and Inclusions

Some scanning electron microscopy and EDAX surface analyses were carried out on post-experiment surfaces. Prior to observation, the plates were washed with absolute ethanol but not wiped. From the limited number of specimens thus analyzed, some interesting observations have been made. A 1500 X SEM photomicrograph of a stylus impression showed what appeared to be an inclusion (dark spot). The inclusion is especially significant in that it appears to have been attacked and significantly altered by the reactants (TCP, E-105, or O_2). EDAX analysis shows principally Fe with traces of P and S in this inclusion. Analysis of stereo pairs of photographs of inclusion pits indicates that the inclusion is essentially decomposed and that it is surrounded by areas of thick film. This observation strongly suggests that the inclusions are nucleation sites for surface reaction. Experiments with zone-refined iron are planned to clarify this point. Similar analyses on the stylus impression show only Fe. A 2100X SEM photomicrograph of a stylus impression in a film formed from pure TCP in 20% O_2/Ar showed some hints of plastic flow and a fractured area suggesting adhesion. Adhesion is indicative of an inefficient film, an observation supported by the low average compressive strengths obtained for the pure TCP film.

The potential role of inclusions was investigated in a series of simple experiments involving the use of inclusion-free zone refined iron surfaces. The experiments were conducted on three substrates, zone-refined iron (ZRI) sputtered on optically flat glass, ZRI sputtered on polished ARMCO and a thick plate of ZRI. In all three experiments, virtually no film of mechanical consequence was formed. In the case of ZRI on ARMCO and the ZRI plate, the temperature was raised incrementally to about 200 C with no evidence of the development of a strong film. Post-test microscope analyses of the

ZRI plate revealed some discoloration in the vicinity of slip planes and plastic deformation resulting from the stylus impression in this soft, large-grained material. The sputtered ZRI surfaces showed a uniform slight discoloration with no obvious stylus impressions.

III. CHEMICAL CHARACTERIZATION OF BOUNDARY FILMS

The rupture strength measurements performed in this program constitute a useful and consistent set of data on the effects of O_2 and H_2O on the formation, stability, and degradation of boundary films formed from TCP-diester solutions. However, as valuable as these data are, they are not sufficient to provide a satisfactory understanding of the physical chemistry of the films. If unambiguous mechanisms are to be determined, supplementary experimental information is needed. Attempts were made in earlier phases of the program to apply ellipsometry to provide such data. These measurements proved to be very useful in corroborating the transitions in the film rupture strengths caused by temperature but could not provide any direct insight into the surface chemistry responsible for these transitions. In order to obtain such chemical information, it became necessary to broaden the scope of the program by applying spectroscopic techniques. Two such techniques were utilized - ESCA (Electron Spectroscopy for Chemical Analysis, also known as XPS, X-Ray Photoelectron Spectroscopy) and FT-IR (Fourier Transform Infrared Spectroscopy).

Electron Spectroscopy

ESCA is an analytical technique in which a specimen contained in an ultrahigh vacuum chamber is irradiated by x-rays, which cause electrons to be ejected from the inner shells of the various atoms in the specimen. These electrons are collected and passed through an analyzer which provides an energy spectrum of the electrons. Such spectra contain peaks characteristic of each of the elements present in the region some 50 to 150 angstroms from the surface. No signal is obtained from electrons deeper in the specimen because of multiple collisons of the ejected electrons which keep them from leaving the specimen. Shifts in the energies of the various peaks in the spectrum can arise from variations in the environment of the atom; that is, shifts due to chemical bonding can be detected.[10] Since extensive work has been done on phosphorus and its compounds,[11] ESCA appears to be a potentially very powerful method for studying the reactions of TCP with iron surfaces. In particular it was hoped to learn the nature of the bonding between the reacted TCP molecules (or fragments) and the ARMCO iron surface by high-resolution ESCA studies of the phosphorous peaks.

Preparation of Specimens

Small ARMCO iron specimens approximately 1 square cm in area and 0.1 cm in thickness were polished by the usual procedure followed for the rupture strength specimens. These were then reacted by heating from 30 minutes to 4 hours in 5% TCP-E105 solutions open to laboratory air (R.H. ca. 50%) at temperatures of 102 C and 150 C. Two specimens were heated at 102 C for 30 minutes, two were reacted at 203 C for 4 hours and two at 150 C for 4 hours. Upon completion of the reaction process each specimen was wicked dry with solvent-

extracted cotton and placed in a vacuum desiccator for several days. ESCA spectra of the residual films were then obtained in a Physical Electronics Incorporated Model 548 ESCA apparatus at the Chemistry Department of The Ohio State University.

Results

Figure 24 is an ESCA spectrum for a specimen reacted at 102 C for 30 minutes. The iron peaks in this spectrum are very weak, indicating that the specimen was covered with a continuous film which effectively prevented the electrons from the iron atoms from escaping the specimen. The strong oxygen peak near 530 eV must be due to oxygen in the organic film rather than from iron oxide. The $C_{(1s)}$ peak near 280 eV may be due to contamination of the specimen or to carbon in the film. Scale expansion (10X) allowed the discernment of several phosphorous and iron peaks and another oxygen peak. The spectra obtained for the specimens treated for 4 hours were found to be virtually identical with the spectrum shown in Figure 24. This indicates that whatever chemical reaction took place must have taken place in the first 30 minutes of exposure of the iron to the TCP-E105 solution.

Figure 25 shows the spectrum of one of the samples reacted for 4 hours at 154 C. This spectrum is very similar to that at Figure 24 except that the Fe peaks are so much weaker that they cannot be distinguished. The scale expanded part of the spectrum shows stronger phosphorus peaks and weaker Fe peaks than the previous spectrum.

In order to observe chemical shifts and thereby obtain information on the binding of the TCP, high resolution spectra of the 154 C specimen were taken in the regions around the $P_{(2s)}$ peak (189.9 eV) and the $P_{(2p)}$ peak (ca 133 eV). Because of a high level of noise the former spectrum yielded no information on chemical

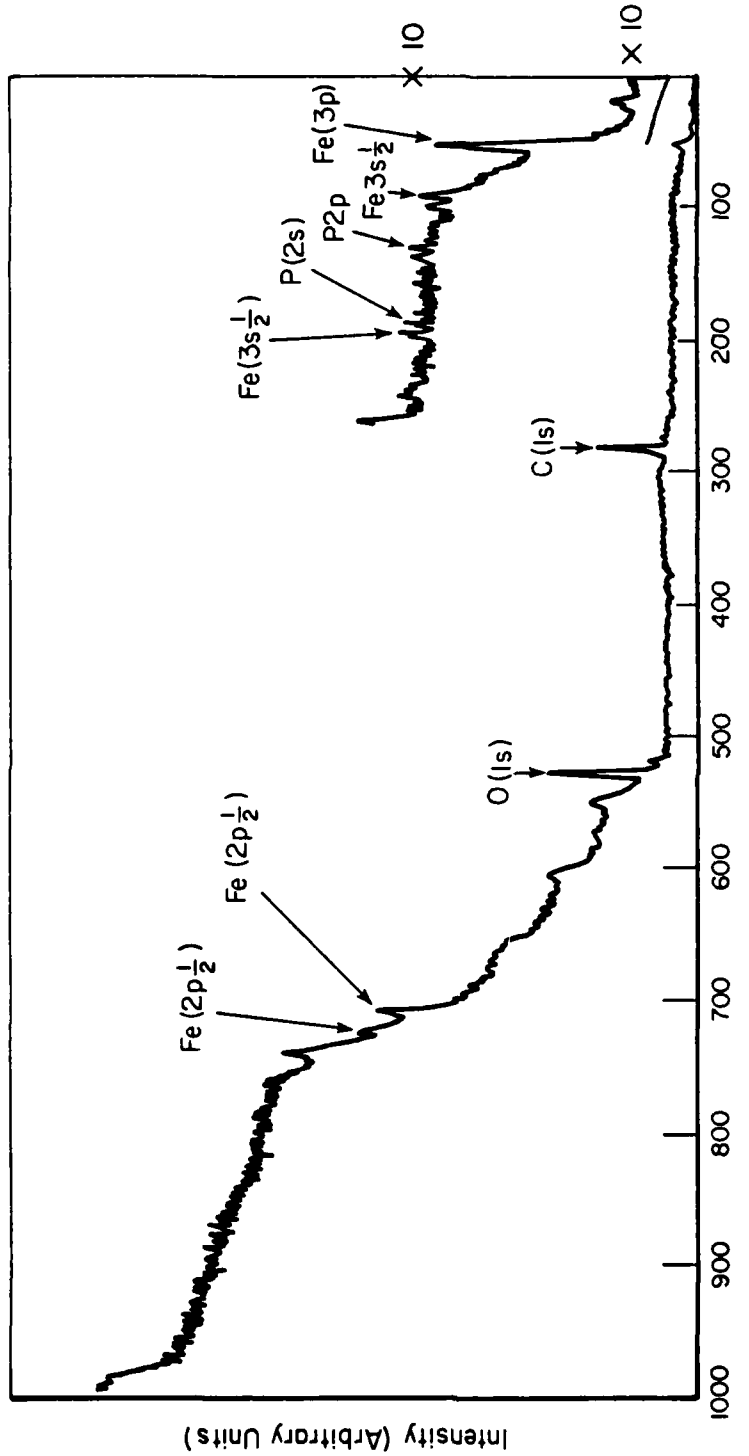

FIGURE 24. ESCA SPECTRUM FOR ARMCO IRON SPECIMEN REACTED AT 102 C FOR 30 MINUTES IN 5% TCP/E105 SOLUTION

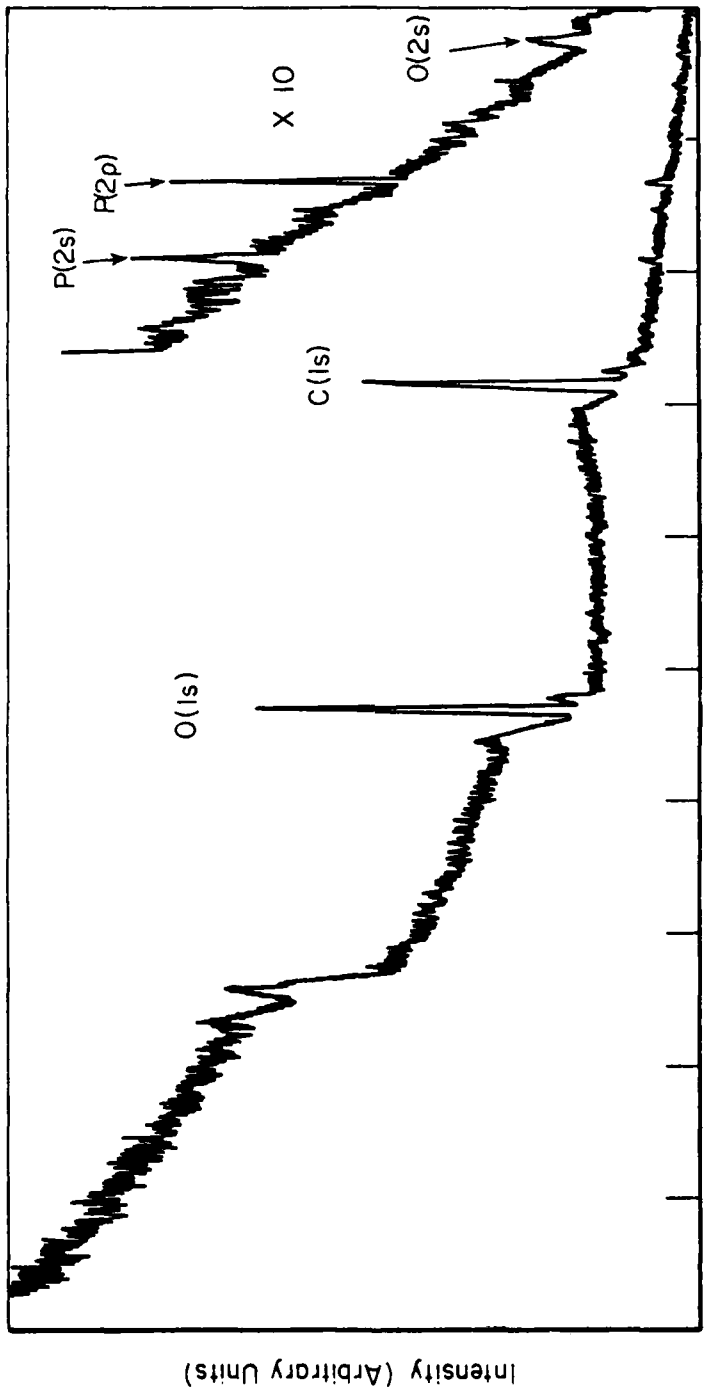

FIGURE 25. ESCA SPECTRUM OF ARMCO IRON REACTED AT 154 C FOR 4 HOURS IN 5% TCP/E105 SOLUTION

shifts. The latter spectrum, given in Figure 26 is much more informative. First, a large shift in the binding energy from elemental phosphorus (E_B = 130.1) is observed since the peak is centered near 133 eV. Unfortunately, the peak is so broad that it is not possible to distinguish among all the possible states in which the phosphorus may be present. For example, E_B for phosphorus in PO_4^{-3} is 132.1 eV for triphenylphosphate, E_B = 133.8 eV, for triphenyl phosphite, E_B = 132.8 eV, and for $P_2O_7^{-4}$, E_B = 133.3 eV.[12] The spectrum in the figure tells us only that phosphorus may be present in all three forms.

At a later time these experiments were repeated on Battelle's newly acquired Leybold-Heraeus LHS-10 ESCA apparatus. This instrument has much better resolving power and better data-handling capability than the instrument used earlier. The same ARMCO specimens were repolished and reacted again in 5% TCP/E-105 solutions. A high-resolution spectrum obtained on the specimen reacted for 4 hours at 154 C is given in Figure 27. As in Figure 26, a large shift in the binding energy from that of elemental phosphorus is observed. Unlike the spectrum of Figure 26, the single peak is quite well resolved and is centered about E_B = 133.9 eV. As mentioned earlier, E_B for triphenyl phosphate is 133.8 eV. The binding energies of tricresyl, monocresyl and dicresyl phosphates would all be expected to lie very close to this value. It is therefore not possible from ESCA spectra to determine which of these species might be present in the surface films produced by the reactions of TCP with ARMCO iron. However, it can be concluded from this work that the films do consist of strongly adsorbed aromatic phosphate compounds. This point will be discussed further in a later section.

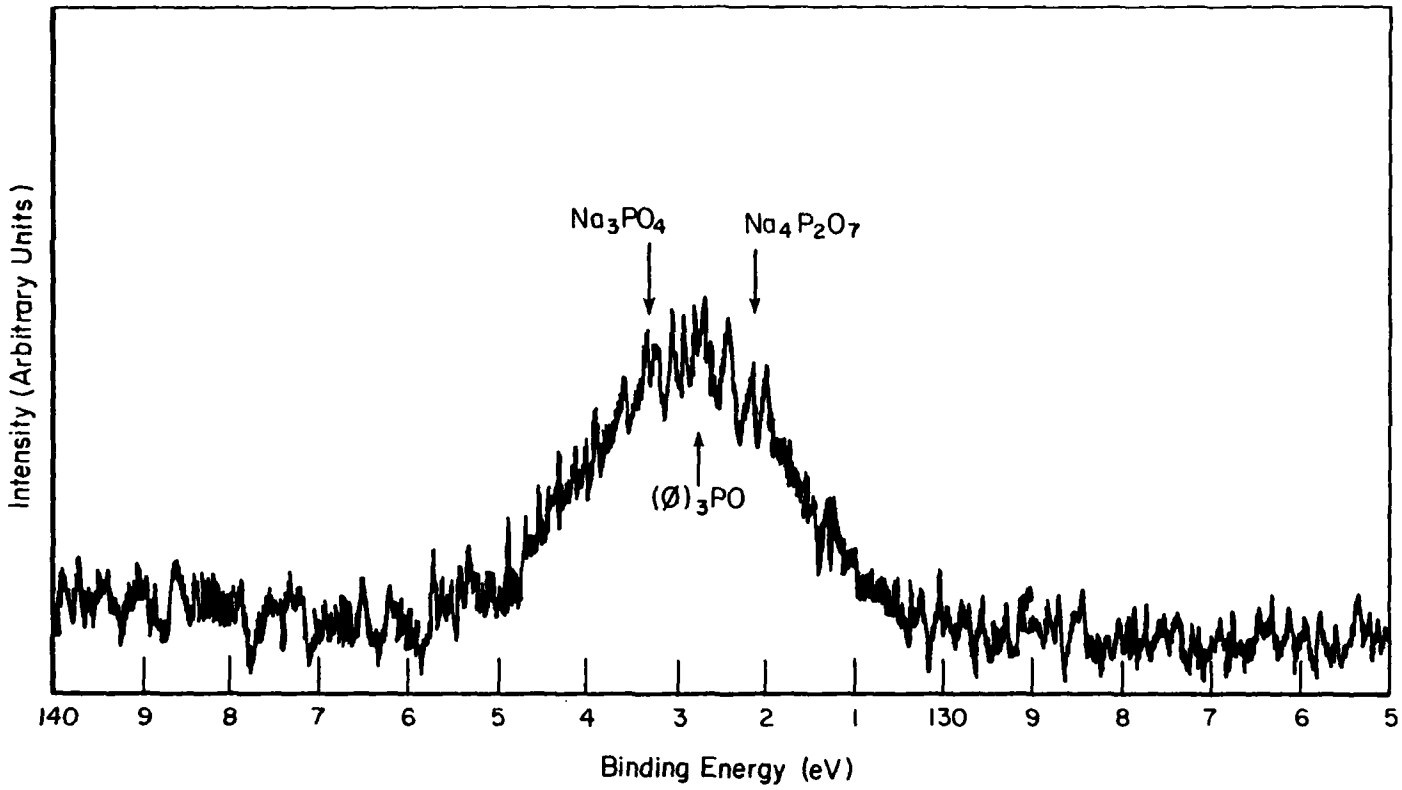

FIGURE 26. PARTIAL HIGH RESOLUTION ESCA SPECTRUM OF ARMCO IRON REACTED AT 154 C FOR 4 HOURS IN 5% TCP/E105 SOLUTION

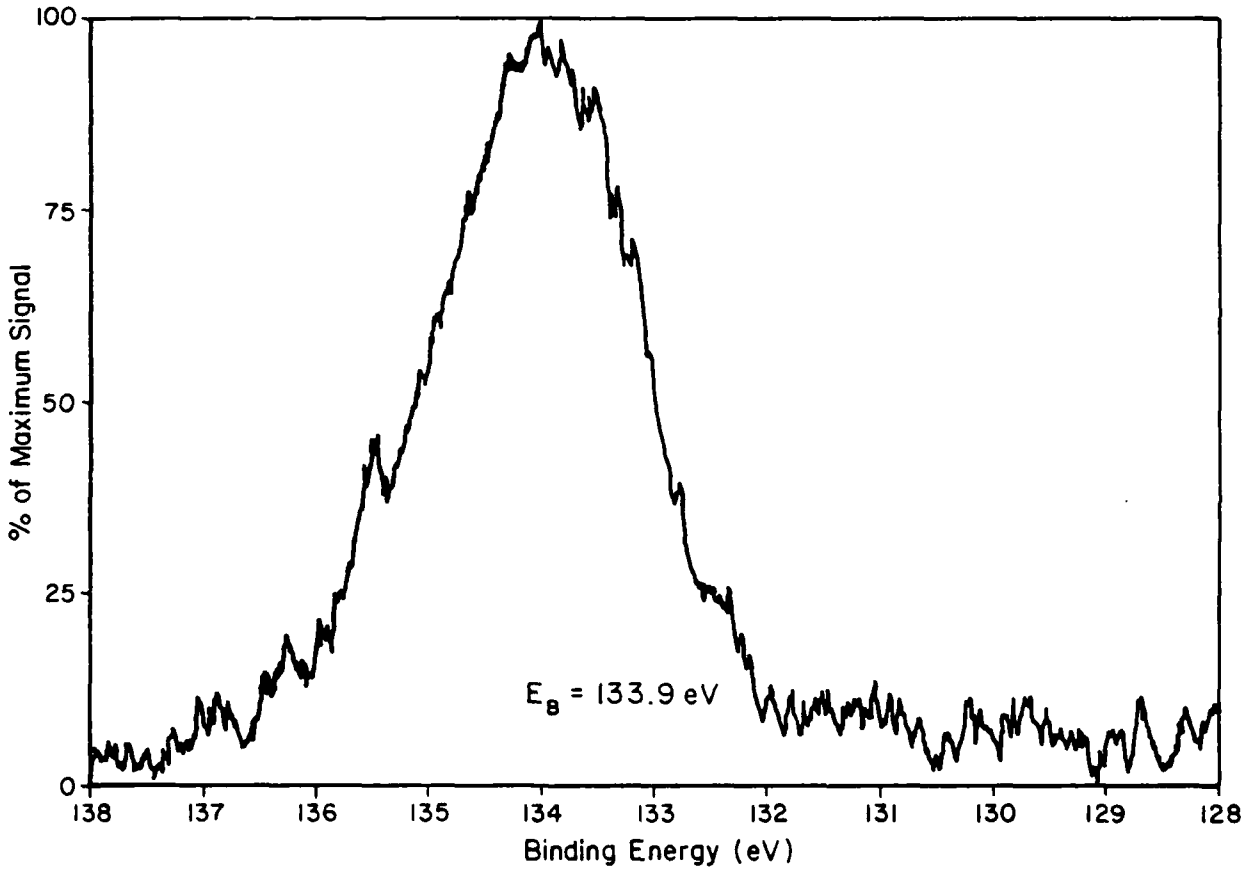

FIGURE 27. HIGH RESOLUTION ESCA SPECTRUM OF ARMCO IRON REACTED AT 154 C FOR 4 HOURS IN 5% TCP/E105 SOLUTION

Fourier Transform Infrared Spectroscopy

Fourier Transform Infrared Spectroscopy (FT-IR) is a highly sensitive spectroscopic technique which differs from conventional dispersive infrared techniques in that the conventional spectrometer uses a monochromator to produce spectral information directly whereas a Michaelson interferometer is used for this purpose in FT-IR.[12] The use of an interferometer to generate spectral information in the form of interferograms requires a dedicated digital computer to perform Fourier transforms of the interferograms (intensity versus retardation) in order to convert them to the usual intensity-versus-frequency spectra. Obtaining spectra in this manner has several advantages. First, it permits substantial gain in light throughput over that obtained in conventional dispersive systems. Further, it has major data-handling advantages in that both interferograms and spectra may be stored in the computer and may be manipulated arithmetically. (For example, spectra may be ratioed, subtracted, or smoothed.) Because of these advantages FT-IR has been used successfully in research on a wide variety of surface and interface problems.[13] Therefore, it is logical to utilize FT-IR in studying the nature of the chemical reactions occurring in the formation of boundary films from TCP-E105 solutions.

Most of the experiments were carried out using a germanium total internal reflection prism coated with a thin film of iron (ca. 1000 A thick) deposited by sputtering from a zone refined iron target (99.999^{+} pure iron). This iron surface was then exposed to either E-105+5% TCP solutions or to pure TCP at 120 C for 10-16 hours. The liquid phase was aerated prior to reaction and the reaction was carried out in an open test tube. The principle behind this experimental approach is to evaluate the IR spectrum of species on the iron surface from the "underside", so to speak. The IR signal passes

through the iron coating (confirmed prior to reaction with the liquid species) and penetrates into the liquid, probably no more than 2-3 molecular diameters.*

The results of the experiments conducted with E-105/TCP solutions were disappointing. The spectra taken before and after reaction at 120 C were virtually identical, with a few tantalizing, but inconclusive, features. Among these was an indication that the P-O stretch frequency was attenuated as a result of the reaction. (Suggesting possible P-O-P formation) In order to improve the signal-to-noise ratio, experiments were carried out with pure TCP. This substantially simplified the spectrum and reduced possible data processing errors due to selective distillation during reaction. As a result, we obtained some reasonably conclusive, but perplexing data: exposure to zone-refined iron at 120 C brought about an increase in P=O and P-O organic peaks and a decrease in cresyl peaks (ring-breathing mode). These seemingly contradictory data can be explained by the limited range of the IR signal in the organic phase. Prior to reaction, the organic phase is randomly-oriented and the IR signal interacts with all sides of the TCP molecule with equal probability. After reaction, the TCP molecules are positioned with their phosphate oxygens oriented toward the Fe surface (closest to the surface) and their aryl groups furthest from the surface. If the range of the IR signal is such that this nominally 40 A distance is a significant fraction of that range, then the results observed are reasonable and indicate the presence of some sort of ordered phosphorus organic array on the surface.

---

* The nominal range of the IR is 2000 A from the Ge surface. The iron will attenuate this somewhat and the surface of interest is 1000 A from the Ge, therefore, 2-3 molecular diameters at a nomainal 40 A per molecule is a reasonable estimate.

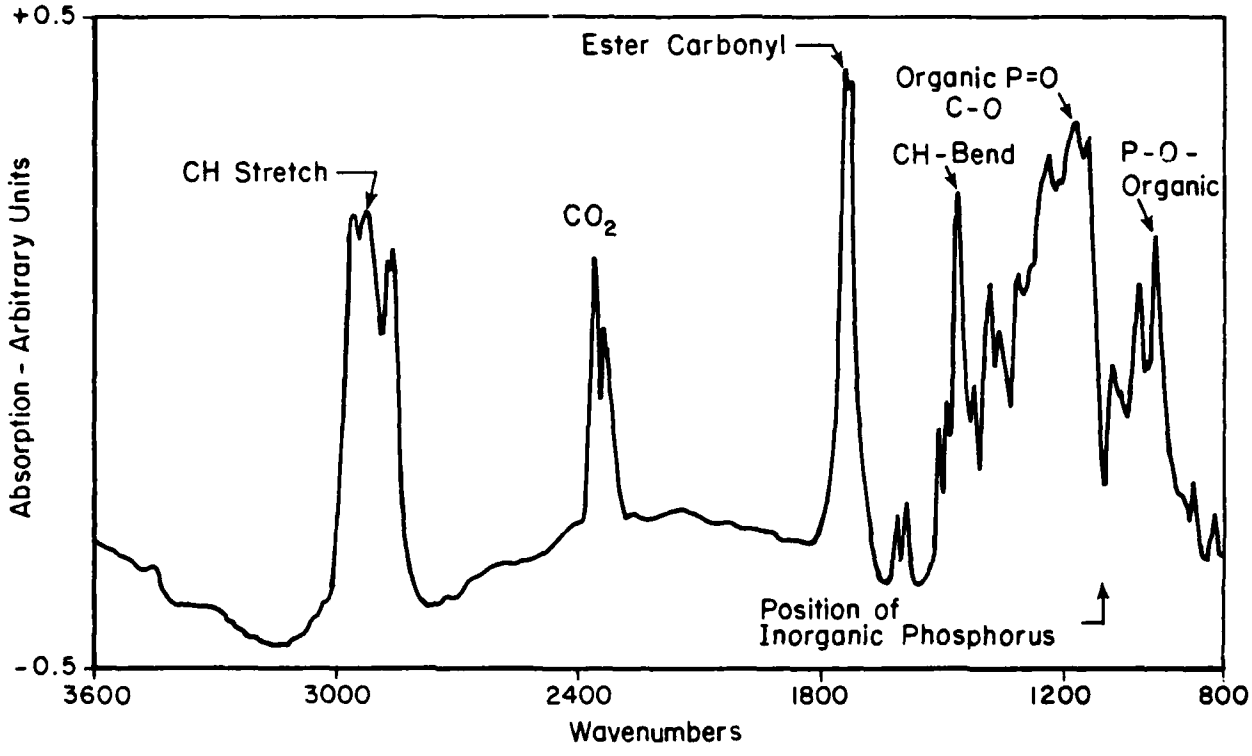

FIGURE 28. EXTERNAL REFLECTION INFRARED SPECTRUM OF ZONE-REFINED IRON PLATE AFTER REACTION WITH TCP/E-105 SOLUTION.

What we do not observe is perhaps more significant than what we do. We see no evidence of inorganic phosphate in any zone-refined iron surface. Further, we see no evidence of a direct Fe-P bond and scant evidence of P-O-P intermolecular bonding. We appear to be dealing with a species that is adsorbed or weakly bound to the iron/iron oxide surface. It is interesting to note that in all cases--solutions and pure TCP--if the specimen is allowed to stand for 2-3 days, it becomes opaque to all IR.

A second, and potentially more useful type of experiment involved direct reflection of an infrared beam off of the highly-polished reaction surface. The iron specimen was prepared in the usual fashion and was reacted with 5 percent TCP in E-105 in an oven for 6 hours at 120 C. The atmosphere was laboratory air. The specimen was drained while it was still hot and placed in the spectrometer immediately upon cooling. The reacted surface was not wiped or rinsed in any way. Two types of experiments were carried out in this manner. They involved ARMCO surfaces and zone-refined iron surfaces.

A typical spectrum is shown in Figure 28. Normalization and subtraction of the spectra obtained using ARMCO surfaces from those resulting from zone refined iron surfaces revealed no significant differences. Further, both spectra showed largely parent species and no evidence of inorganic phosphorous.

Wash Experiments

All of the reflectance experiments gave strong spectra from the parent compounds--E-105 and TCP--from which we endeavored to extract indications of small changes. In an effort to reduce the possible interference of the parent spectral components with the sought-after reaction products, we conducted a series of experiments where the reacted plate was rinsed with hexane and/or methyl alcohol prior to obtaining the infrared spectra.

Experiments were carried out on ARMCO plates reacted with 5 percent TCP/E-105 solutions in laboratory air at two temperature levels: 120 C and 200 C. Reflectance spectra were taken from the bare ARMCO plate rinsed with solvent and dried, the plate dipped in an E-105/TCP solution, the same plate reacted and drained of excess liquid, and that plate rinsed with ethanol and hexane. (Post-wash spectra indicated that the two solvents had identical effects.)

Comparisons of spectra from pre- and post-reacted surfaces indicate a solvent-resistant peak at about 1200 wave numbers in the case of reaction at 120 C and a significant shift toward lower wave number-- ca 1000-900--for components of the spectra from a rinsed plate reacted at 200 C. The higher wave numbers indicate organic phosphate, while the lower indicates inorganic phosphate. The spectra from the higher temperature reaction showed some evidence of residual organic phosphate; however, the spectra from the low temperature reaction showed little, if any, evidence of inorganic phosphate.

These data suggest that at low reaction temperatures, an organic film containing phosphate is formed and that at higher temperatures either this film is converted to an inorganic form or an inorganic film is formed from the onset.

Bulk Experiments

The results of the analyses of thin surface films may be interpreted in two ways: either no unique chemical surface species result from the interaction of TCP ester species and the iron surfaces at the temperatures employed, or these species are below the limits of detection of the methods employed. Bulk experiments using relatively large quantities of liquid reactants and large iron surface areas offer the possibility of determining, at least, the chemical processes taking place in the bulk liquids under various condi-

tions of moisture, oxygen and temperature. Of particular interest are the potential effects of oxygen on the ester and/or TCP in the liquid phase.

To this end relatively large volumes of TCP/E105 solutions were subjected to temperatures of 120 C in the presence of ARMCO iron filings, zone-refined iron filings, and air or argon. The experiments were carried out as follows:

Approximately 50 ml of solution were placed in a large test tube along with a quantity of iron filings that had been carefully degreased (heptane and absolute ethanol), etched with diluted HCl, washed with distilled H_2O and oven-dried overnight. The tube was fitted with a glass bubbler and the assembly placed in a convection oven maintained at 120 $\pm$ 2 C. Either dry air or argon was bubbled at a very slow ($\sim$1 bubble/second) rate for the duration of the reaction. The reaction was allowed to proceed for 20 hours, after which the liquid phase was analyzed for total acid number by means of ASTM D664, and was subjected to fourier-transform infrared (FTIR) analyses. In addition, FTIR analyses were employed to characterize species on the surface of the solid phase.

Table 3 summarizes the results of the acid number experiments.

These data indicate that oxygen is responsible for the production of an acidic species. This species may be directly related to the surface film or may be a by-product of a reaction leading to the production of strong films.

The infrared analyses indicated the presence of a phosphorus-containing aromatic (other than TCP) in the bulk fluid exposed to ARMCO iron (#3 in Table 3) and, possibly, a trace of free carboxylic acid in the bulk fluid exposed to zone-refined iron. (#4, Table 3). The fluid exposed to ARMCO iron did not show this evidence of carboxylic acid. The ARMCO surfaces from experiment #3, Table 3, showed only one new component, (that is other than TCP or E-105) an

TABLE 3. BULK EXPERIMENTS - CONDITIONS AND ACID NUMBER OF RESULTING LIQUID PHASE (all experiments carried out at 120 C for 20 hours)

Exp #	Liquid Phase	Solid Phase	Atmosphere	Temp, C	Total Acid # of Post Exp Liquid Phase
1	5% TCP+E105	None	Air	25	0.245
2	E-105 neat	ARMCO Fe	"	120	16.2
3	5% TCP+E105	"	"	120	8.3
4	5% TCP+E105	Zone-Refined Fe	"	120	8.3
5	5% TCP+E105	None	"	120	0.25
6	5% TCP+E105	ARMCO Fe	Argon	120	0.48

ester with a possible ether link. No evidence of inorganic phosphates or metal soaps was noted in contrast to earlier observations. The infrared analyses of fluid solutions heated to 120 C in the absence of oxygen and/or iron showed essentially parent species.

IV. DISCUSSION

Summary of Results

Our overall observations may be conveniently summarized in terms of the influence of the variables studied on the mechanical properties of the surface films.

Effects of Temperature:

- Films formed from the pure ester increase in strength up to temperatures of 100 C. The compressive strength then begins to fall off and collapses entirely at temperature levels above 200 C.

- Films formed from solutions of TCP in the ester do not begin to develop significant strength until temperatures of the order of 110 C are reached. Those films increase greatly in strength at temperatures above 150 C and do not show evidence of loss of strength at temperatures of up to 204 C.

---

* This analysis was accomplished by incorporating the reacted iron turnings into a KBr pellet. A standard transmission fourier transform infrared analysis was then conducted.

Effects of water:

- Water leads to weakened films at temperatures below 100 C and has little effect at temperatures above 100C. Both ester and TCP/ester films are similarily effected.

Effects of Oxygen:

- The presence of oxygen is essential to the formation of compressively-strong films.

- The strength of films formed from TCP/ester solutions is independent of oxygen concentration in the atmosphere above the film and dissolved in the solution for oxygen concentrations above 5 percent by volume. Below this concentration, the system behaves essentially as though no oxygen were present.

- In bulk experiments, the acid number of nominally oxygen-free, argon-saturated solution after reaction with iron filings is very low.

Effects of TCP Concentration:

- The rate of increase of film strength is independent of TCP concentration.

- The time required for the onset of the development of significant strength is strongly influenced by the concentration of TCP. This induction period is at a minimum at concentrations around 5 percent (vol.) TCP in

E-105 and a maximum at 100 percent TCP.

Effects of Substrate:

- Films formed on ARMCO surfaces are significantly stronger than those formed on ultra-pure, zone-refined iron surfaces.

- The acid number of bulk TCP/E-105 liquid solutions exposed at temperature to zone-refined iron filings is lower than that of solutions exposed to ARMCO iron filings.

- The acid number of solutions exposed to heat and air in the absence of iron is unchanged from the pre-exposure condition.

Conclusions

As a result of the large volume of data obtained under a variety of conditions using a variety of techniques, it is possible to conceive a general working hypothesis which is useful for structuring the discussion of these data. Furthermore, this hypothesis, although by no means a complete elucidation of the detailed mechanisms of the interaction of TCP with iron, points the way to further research. This working hypothesis involves two general steps as follows:

(1) A relatively weak precursor film, completely organic, is formed over the entire iron surface. This film is probably TCP (unreacted or only partially reacted)

adsorbed and oriented on the Fe/Fe oxide surface, with some degree of order; because of the weakness of the interaction between TCP and the substrate in this precursor stage, the infrared and ESCA spectra cannot be distinguished from those of the parent compound, even though the TCP may be adsorbed at polar sites. The retarding effect of water on film formation can be explained on the basis that the TCP must compete with water, which is thermodynamically favored, in order to become adsorbed at such sites.

(2) The precursor film is transformed locally by an oxidative process into a strong, inorganic films containing phosphorus, probably as a phosphate. Nonmetallic inclusions, or perhaps some other unrecognized feature on the ARMCO surfaces, enter into this process in some way--directly or catalytically. The oxidative process takes place slowly at lower temperatures, accelerating as the temperature increases.

The transformation into a strong film is not possible in the absence of oxygen and is greatly retarded or not possible in the case of zone-refined iron surfaces. The role of the inclusions on the ARMCO surface is not clear; however, the experiments of rupture strength versus time then show a considerable scatter in the data in the post-induction time period, suggesting a nonuniform film forming perhaps at the inclusions and spreading across the surface.

One is tempted to attribute the low slope portion of a typical load-time curve (see, for example, Figure 23) to the adsorbed organic film and the high slope portion to the transformation into a stronger, inorganic film. We have little direct evidence to support this, and more IR experiments at low temperatures where the "organic"

film dominates and high temperatures where the "inorganic" film dominates are indicated.

The oxidative process operates either on the adsorbed film, on the bulk liquid, or on both. The experiment depicted in Figure 22 shows the effect of the introduction of O_2 into a system where a weak "organic" film has been established. The shape of the curve suggests a diffusion process and oxidation of the film in situ.

The oxygen concentration threshold effect could be related to the competing reaction of O_2 + Fe Fe (oxides). This reaction is thermodynamically favored over all other possibilities and the lower concentration of oxygen may be completely consumed in satisfy- ing the needs of this process. Above 5 percent O_2 there is sufficient oxygen available to allow the process of the oxidation of the adsorbed film.

LIST OF PUBLICATIONS RESULTING FROM THIS RESEARCH

1. Drauglis, E. J. and Snediker, D. K., "The Role of Inclusions in the Formation of Boundary Films on Iron Surfaces", Wear 61 (393), 1980.

LIST OF PROFESSIONAL PERSONNEL ASSOCIATED WITH THIS PROJECT

1. E. J. Drauglis, Ph.D., Surface Chemistry and Analysis
2. D. K. Snediker, Ph.D., Mechanical Properties
3. S. Winter, Fourier Transform Infrared Analysis

REFERENCES

(1) Buckley, D. H., "Oxygen and Sulfur Interactions With a Clean, Iron Surface, and the Effect of Rubbing Contact On These Interactions", Preprint No. 73LC-5B-4, ASLE/ASME Joint Lubrication Conference, October, 1973.

(2) Fein, R. S., Kreuz, K. L., and Rand, S. J., "Solubilization Effects in Boundary Lubrication", Wear 23 (393), 1973.

(3) Begelinger, A. and DeGee, A.W.J., "Boundary Lubrication of Sliding Concentrated Steel Contact", Wear 22 (337), 1972.

(4) Schatzberg, P., "Influence of Water and Oxygen in Lubricants on Sliding Wear", Lub. Eng., p. 301, September, 1970.

(5) Beerbower, A., "Boundary Lubrication", AD747336, Scientific and Technical Applications Forecast, Chief of Research and Development, Department of the Army Washington, D.C., 1972.

(6) Matveevskiy, R. M. and Buyanovskiy, I. A., "Effect of Alloying Steel with Chromium on the Thermal Stability of Lubricating Boundary Layers", Mashinovedenie 4 (108), 1970.

(7) Rebinder, P. A. and Shchukin, E. D., "Surface Phenomena in Solids During the Course of Their Deformation and Failure", Usp. Fiz. Nauk 108 (3), 1972.

(8) Kannel, J. W. and Snediker, D. K., "Characterization of Boundary Lubrication Films Using a Rupture-Strength Criterion", Wear 30 (105), 1974.

(9) Llopis, J., et al ., "Surface Reaction of Iron With Thio- and Phosphorus-Organic Compounds Dissolved in Hydrocarbons" - Report to U.S. Air Force AFSC, AFEOAR 61(052)-523, AD412357, April, 1963.

(10) Kane, P. F. and Larrabee, G. B., Eds., Characterization of Solid Surfaces Plenum Press, New York, 1974, p 307.

(11) Carlson, T. A., Photoelectron and Auger Spectroscopy , Plenum Press, New York, 1975, p. 356.

(12) Griffin, P. R., Chemical Infrared Fourier Transform Spectroscopy , John Wiley, New York, 1975.

(13) Jakobsen, R. J. in Fourier Transform Infrared Spectroscopy , J. R. Ferraro, Ed., Academic Press, New York, 1978, p. 165.

(14) Shafrin, E. G. and Murday J. S., "Analytical Approach to Ball-Bearing Surface Chemistry", J. Vac. Sci. Technology 14 , 246 (1977).

APPENDIX A

CYCLIC DEFORMATION AND FATIGUE DAMAGE STUDIES

APPENDIX A

CYCLIC DEFORMATION AND FATIGUE DAMAGE STUDIES

Introduction

Surface chemistry may dictate the utility of a given lubricant in a given service environment. Prior sections of this report have examined this aspect in the context of service environments for which the mechanical loading is quasi-static--specifically zero. These studies examine but one facet of the wear/lubrication problem. Many others exist in the more realistic service environments which involve steady or more typically repeated cyclic mechanical loads. One often observed form of such wear phenomena is fretting-fatigue which develops when metallic surfaces in contact are also subject to cyclic mechanical loads. Unfortunately, these processes appear to be very complex and, as yet, no general theory has evolved.[A1] Engineers, therefore, must rely on what empirical data exist.

This section of the report presents the results of a first rather tentative and small step taken in an effort to unravel the complexity of the interaction between surface chemistry and mechanical behavior. The focus is on the influence of surface chemistry on both the cyclic stress-strain behavior of a metal and its fatigue resistance. Notice that as the prior sections of the report bounded such complex phenomenon as fretting-fatigue at the limit dominated by surface chemistry, this segment examines the limit dominated by mechanical behavior. As these limiting processes are understood, the range of problems that lie between them can be approached and explored from a knowledge base gained at these limits.

Specifically, the objective of this limited study was to assess the interaction between surface chemistry and mechanical behavior as manifest in changes in cyclic deformation response and fatigue crack initiation and growth via empirical observation. The scope of the study was quite restricted in that it is probing areas

which have not been extensively explored in the previous literature. Cyclic deformation and fatigue crack initiation and propagation data have been developed from tests of rather small samples loaded under constant amplitude cyclic strain control. Details of the experiments and results and discussion follow in sections entitled "Approach; Experimental Aspects and Program; Results and Discussion; and Conclusions and Recommendations."

Approach

The approach consisted of comparison testing similar samples subjected to identical loadings in either air or lubricant.* In both cases, testing was done at 130 C. After testing, the relative influence of surface reactions could be assessed by comparing results in terms of (1) stress response with cycles and (2) cycles to crack initiation and specimen failure. While more elaborate programs might explore this behavior at notches and crack tips under more general loadings, this limited program examined it in the simple context of uniaxial specimens subjected to fully reversed strain cycling at 0.35 Hz. Moderate strains were used to expedite testing which developed the two necessary conditions for fatigue--local cyclic inelastic strain and a tensile stress. Likewise, these tests provide for the continuous generation of new (microcrack) surface where slip bands created by the reversed inelastic loading intersect the free surface, to sustain the surface--chemistry activity. In summary, the approach is empirical with conclusions to be drawn on the basis of comparison testing.

---

* The lubricant is as described earlier.

Experimental Aspects and Program

Material and Specimen

The material used in this investigation was a hot rolled, high purity 0.02% C iron slightly different form the ARMCO iron used in the surface chemistry studies. It was obtained in the form of blanks about 2-1/2 x 2-1/2 x 0.35 inch in size from ingot iron supplies on hand at Battelle. The material showed a very uniform microstructure in three dimensions. Figure A-1 is a view typical of this microstructure whereas Table A-1 presents the chemistry.

Figure A-2 shows the plan form of specimen geometry used. Note that the test section is rectangular, the specimen thickness being about 0.345 inch thick. In an attempt to avoid gage length-shoulder transition failures (i.e., confine failures to gage section), the gage section was tapered centrally from the shoulders to a maximum reduction of 0.005 inch. All surfaces in and near the gage section were mechanically polished after machining to a finish of about 16 microinches rms. After polishing, they were oiled and remained in that state until testing, at which time they were cleaned.

Apparatus and Method

All tests were conducted in a closed loop-servocontrolled electrohydraulic machine. Specimens were axially loaded under indirect strain control. Load was monitored by a load cell mounted in series with the specimen. Temperature was close-loop controlled with respect to thermal couples on the specimen's shoulders. Heating to a constant 130 C was achieved through heating tape wrapped around grip

TABLE A-1. COMPOSITION OF HIGH PURITY IRON

Element	Weight, %
C	0.02
Mn	0.061
P	0.003
S	0.013
Si	0.001
Cu	0.021
Sn	0.001
Ni	0.007
Cr	0.006
Mo	0.000
Al	0.009
V	0.000
Cb	0.002
Zr	0.001
Ti	0.000
B	0.0000
Co	0.000
W	0.00
Pb	0.00

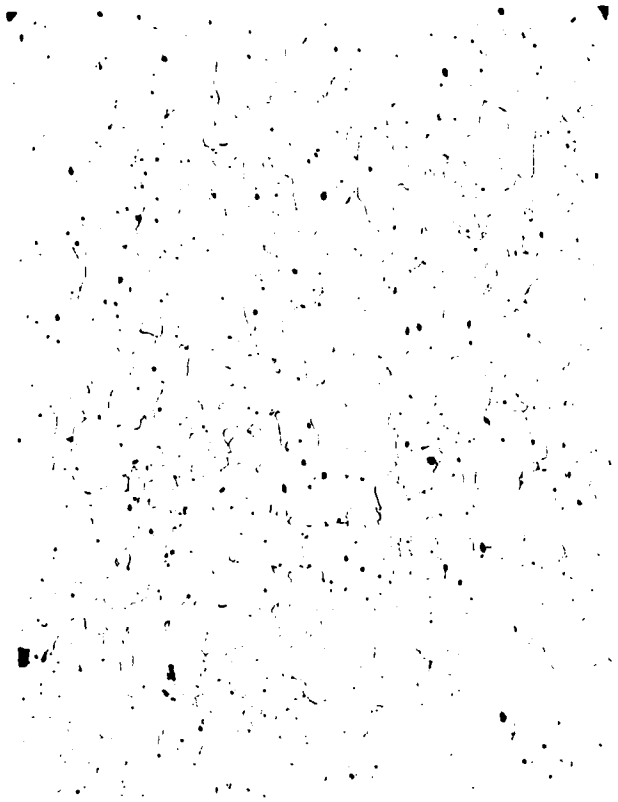

100X Optical 1K208

FIGURE A-1. TYPICAL MICROSTRUCTURE

(Blank Face/2 % nital)

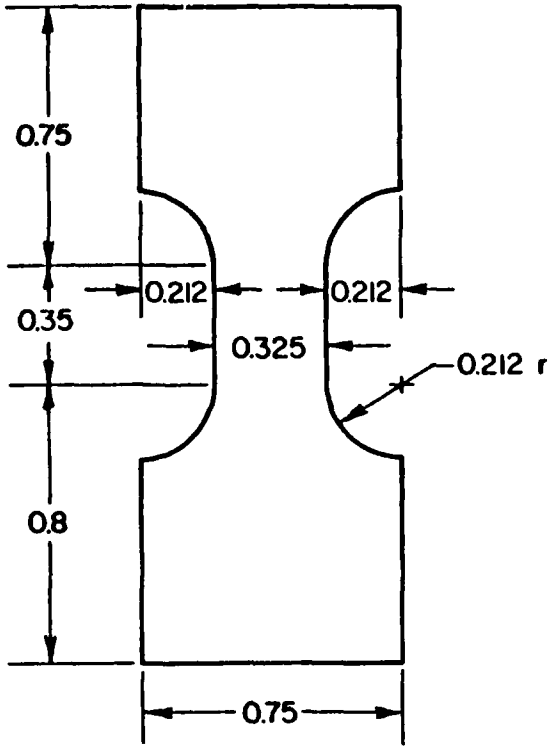

Note: All dimensions in inches.

FIGURE A-2. PLAN FORM OF SPECIMEN

fixtures, the specimen being heated via conduction. This technique was applied in all tests.

Testing was conducted either in ambient air or lubricant.* The air environment was 20 C with a 50 percent relative humdity. Testing in lubricant was accomplished by mounting a lexan chamber sealed to the shoulders of the specimen via silicone rubber.** The chamber enclosed the entire gage section and a portion of the shoulders with static lubricant which was changed with each test. The chamber was filled just prior to starting a test. A view of the specimen is shown in Figure A-3.

As noted above, all tests were done in srain control. For tests conducted in air, strain was controlled by means of a clip-on extensometer calibrated to ASTM Class B_1. That is strain control for the "in air" tests was achieved by controlling the displacement over a fixed gage length. Because of the taper, however, the strain is not uniform over this length. For this reason, two specimens were instrumented with short gage length strain gages and subjected to the incremental strain history shown in Figure A-4(A-2) to calibrate displacement against strain at the anticipated failure location.

Notice that by analogy to the data of Figure A-4, this history will develop nested displacement--strain gage and stress

---

* The lubricant used is that described earlier.

** The combination of lexane and silicone rubber were selected from several possible combinations, based on a study of compatibility and integrity under the test conditions.

4531-1

FIGURE A-3. VIEW OF THE CHAMBER AND SPECIMEN

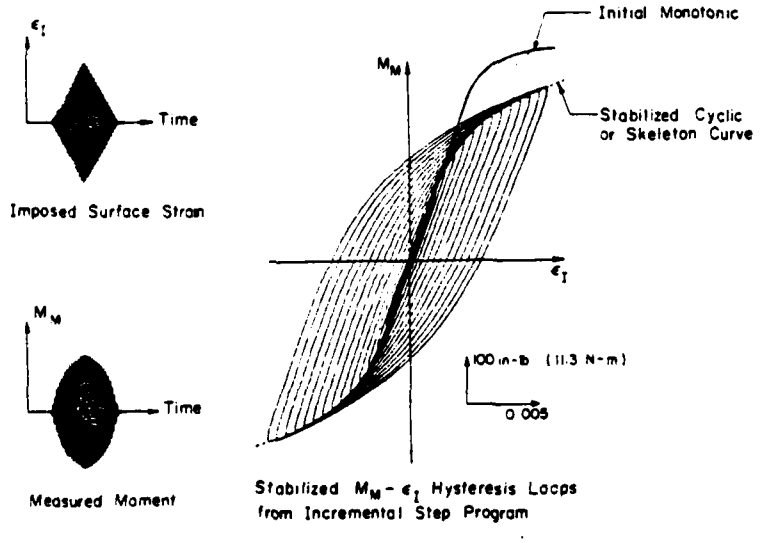

FIGURE A-4. INCREMENTAL STRAIN HISTORY AND RESULTING STRESS-STRAIN BEHAVIOR

(load)--strain gage hysteresis loops. The former provide for indirectly controlling strain via displacement whereas the latter develops the cyclic stress-strain curve for this materials. In both cases, the information sought is defined by the locus of nested loop-tips, the results of which are plotted in Figures A-5 and A-6, for the displacement-strain calibration and the stress-strain curve, respectively. Also shown in Figure A-6 are results developed from the more usual tensile test and from fatigue tests, as discussed later.

In contrast to the "in air" tests for which strain could be indirectly controlled in terms of displacement by a clip-on extensometer the chamber used for "in oil" tests precluded extensometry attached to the gage section. For these tests, strain gage strain in the gage section was monitored as a function of specimen extension or stroke, the calibration being derived from samples tested in air. Again, an incremental history was imposed so that now the stroke-strain calibration can be developed from the loop tips of nested stroke-strain hysteresis loops. Alternately, it can be derived by cross plotting results of displacement-strain and displacement-stroke to eliminate the extensometer (displacement) results of which were used in this program and have been presented in Figures A-5 and A-7. Note that these calibration curves were symmetric in tension and compression and essentially invariant with cycles, as has been shown for example in Figure A-7.

In all tests, the procedure was to set up the specimen in load control aafter which the appropriate value of the control variable to achieve a given strain was selected and programmed. Control was then shifted to either displacement or stroke, as appropriate, and cycling commenced.

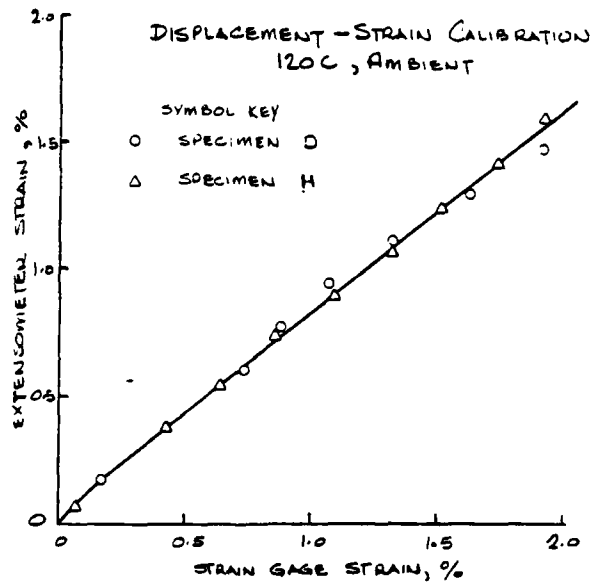

FIGURE A-5. DISPLACEMENT-STRAIN CALIBRATION DATA

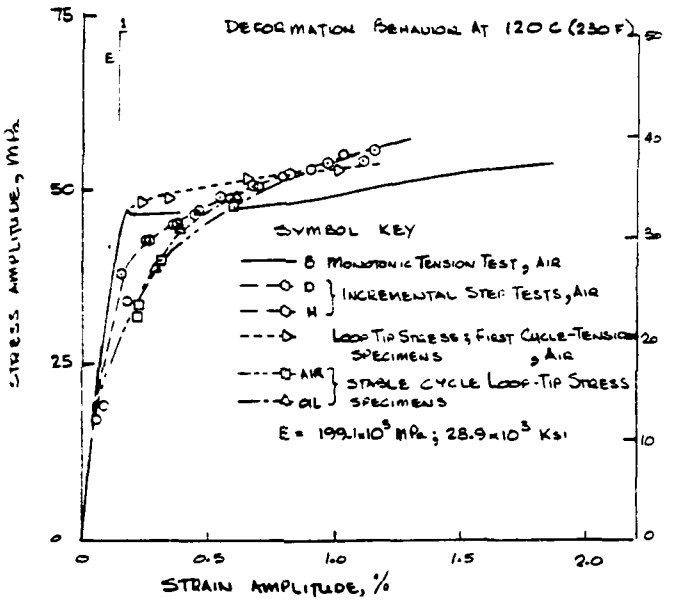

FIGURE A-6. DEFORMATION RESPONSE

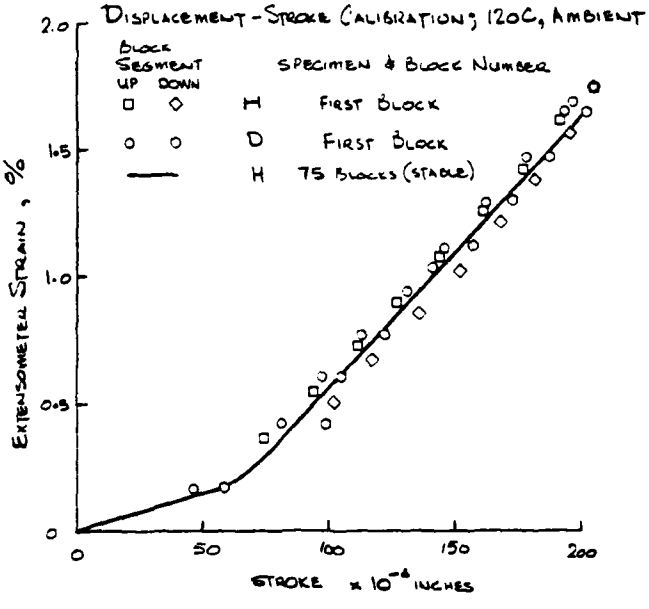

FIGURE A-7. DISPLACEMENT-STROKE CALIBRATION DATA

Experimental Program

A total of 12 specimens have been used in this rather limited study. One was used to develop the monotonic stress-stain curve and related material properties. Two others were used to establish calibration between extensometer displacement, stroke, and strain gage strain. Four specimens were used to develop "in air" data whereas the remaining five were tested "in oil". Table A-2 indicates the distribution of specimens.

Results and Discussion

Results developed in this program focus on the deformation and fatigue resistance of the test materials. They are presented in that context.

Deformation Behavior

The deformation behavior exhibited by this material has been presented in Figure A-6. With reference to the symbol key, note that the monotonic stress strain behavior differs from that developed under fatigue cycling. Further note that the monotonic results differ from data developed from even the first cycle of fatigue testing. These differences, known as cyclic hardening if the stress response increases and cyclic softening if it decreases, are due to cycle induced changes in the dislocation density and morphology. They are typical of most engineering materials.

More significant in the present study is the fact that the stable cyclic deformation behavior differs in air as compared to oil. With reference to the figure, note the curve for tests carried out in oil, designated by the open squares. Such a result is not ex-

TABLE A-2. EXPERIMENTAL PROGRAM

Specimen	Purpose	Environment[a]
B	Tension Test	Air[b]
C	Fatigue	Air[b]
D	Calibration	Air[b]
E	Fatigue	Air[b]
F	Fatigue	Air[b]
G	Fatigue	Air[b]
H	Calibration	Air[b]
I	Fatigue	Oil[c]
J	Fatigue	Oil[c]
U	Fatigue	Oil[c]
X	Fatigue	Oil[c]
Y	Fatigue	Oil[c]

(a) All tests done at 130 C in strain control.

(b) 20 C and 50 percent relative humidity.

(c) Same make-up as used in surface chemistry study.

pected on the basis of prior studies which have typically not discussed this aspect presumably because those tests were done in load-control but neither strain nor stroke was monitored (e.g. (A-3)). This trend is evident in all data developed, becoming quite pro- nounced at larger strains. In all cases, the response is symmetric in tension and compression.

Differences in stress response shown in Figure A-6 reflect the stress for a given strain at one-half of the total life of the specimen. Typically considered as representing the stable cyclic stress of a material under controlled strain cycling, the results shown in Figure A-8 suggest that this material does not stabilize with cycling. This is evident in the figure in that the stress does not tend to a constant value with cycles. Differences discussed above in the context of Figure A-5, therefore, may be due to differences in the rates of change in these stress transients. More fundamentally, they may be due to an interaction between the environment and dislocations which intersect the surface. Since fatigue damage concentrates at the surface, any environmental interaction which pins dislocations would cause an increased stress for a given strain which increased, as observed, with strain amplitude (cf Figure A-5). Presently, too little data are available to examine this observation beyond the just noted speculation.

Fatigue Resistance

Study of the fatigue resistance of these test pieces indicated that, even at the large strains considered, the life of the specimen is dominated by the nucleation and growth of microcracks. Results indicated less than 10 percent of the total life is spent growing an initiated crack about 0.01 inch long to (a macrocrack) failure. As such, this study primarily characterizes the influence of the lubricant on the crack nucleation and microcrack growth

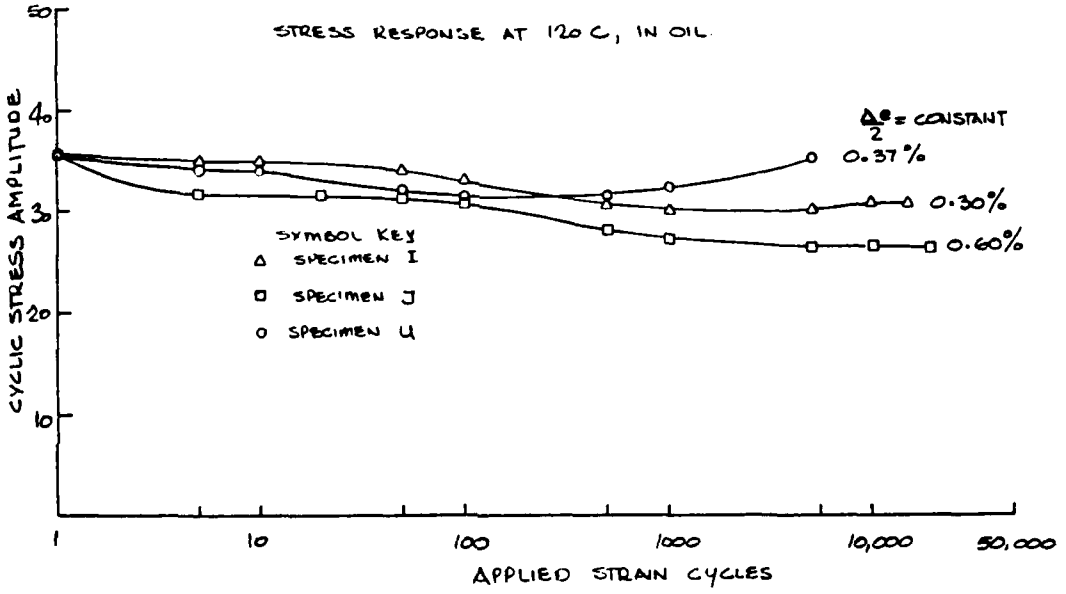

FIGURE A-8. STRESS RESPONSE AS A FUNCTION OF APPLIED STRAIN CYCLES

process.

A total of 9 comparative tests have been done, the results of which are plotted in Figure A-9. Data developed in air are shown as open upright triangles whereas that developed in oil is shown as inverted triangles. Note here that the ordinate is a function with units of stress and the abscissa is cycles to failure. This function is introduced to account for the fact that failures in air occurred in the gage section as anticipated whereas those in oil occurred at the shoulder transiton. As explained in Figure A-10, this function provides an equivalence between the stresses and strains at the two failure sites thereby permitting direct comparison of these two data sets.

With regard to the data shown in Figure A-9, note that at the higher strain and shorter exposure time, the test results for air and oil compare almost identically. However, at lower strains and longer exposure times, the oil and air results diverge significantly. The fatigue resistance in oil is substantially reduced as compared to tests in air, a trend which if continued into the endurance regime could result in order of magnitude differences. Again, this result is new in the sense that oil has been always considered a benign environment. However, it appears that a surface acceleration of initiation is occurring, perhaps due to an attack of inclusions or other constituent in a surface chemistry reaction.

Conclusions and Recommendations

The results of this study demonstrate a clear and very strong tie between the surface activity of this lubricant and the cyclic deformation and fatigue and fracture behavior of a pure iron. The ramifications of such interactions are sweeping in that it has long been believed that such enviroments are benign. Unfortunately, the results presented are limited in both scope and quantity. Fur-

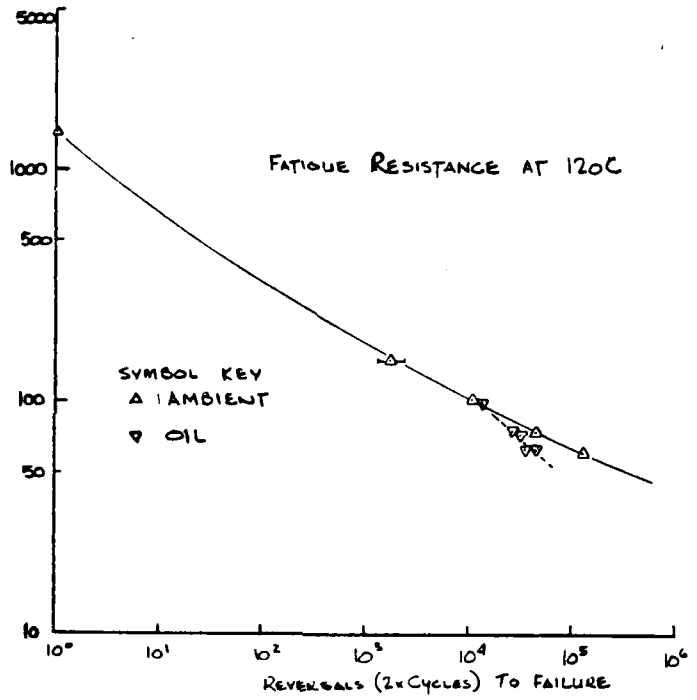

FIGURE A-9. FATIGUE RESISTANCE IN AIR VERSUS OIL

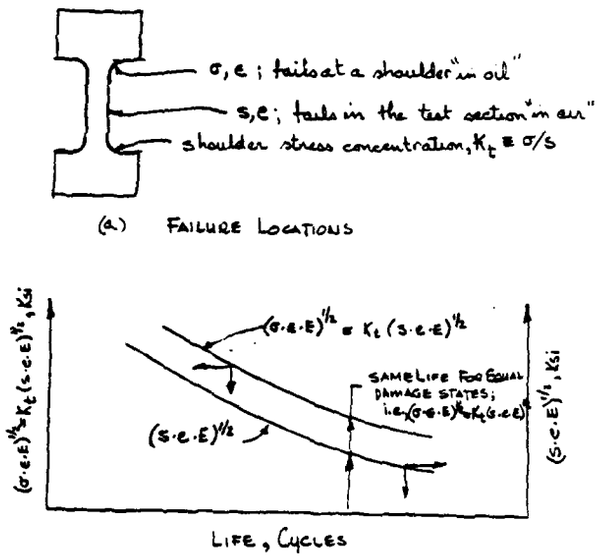

FIGURE A-10. SCHEMATIC OF DAMAGE EQUIVALENCE AND FAILURE LOCATIONS

ther probing of the fractography and surface changes induced by the environment are appropriate as is an expanded format involving a broader testing program.

REFERENCES

A-1. Waterhouse, R. B., Fretting Corrosion, Pergamon, 1972.

A-2. Williams, D. P., Lind, N. C., Conle, F. A., Topper, T. H. and Leis, B. N., "Structural Cyclic Deformation Response Modeling", Proceedings of the ASCE Specialty Conference on Engineering Mechanics, May, 1976, in Mechanics in Engineering, University of Waterloo Press, 1977, pp 291-311.

A-3. Frost, W. T., and Burns, D. T., "Effect of Oil and Mercury at High Pressure on the Fatigue Behavior of Thick-Walled Cylinders of EN-25", Proceedings of IME, Vol. 182, Part 3C, 1967.

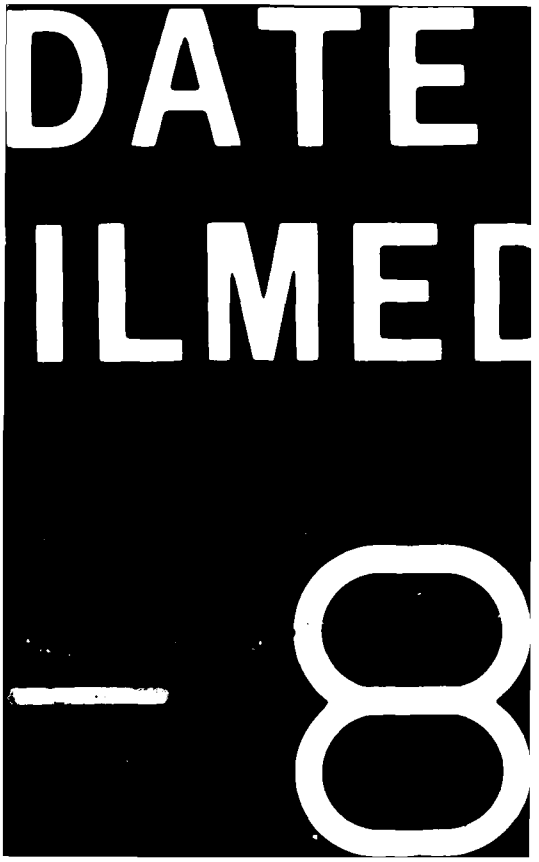
DATE
ILMED
8